Pacific Northwest
NATIONAL LABORATORY

PNNL-33736

# Gap Analysis on the Impacts of Hydrogen Addition to the North American Natural Gas Infrastructure Polyethylene Pipelines

July 2022


Kevin L. Simmons
Lisa Fring
Wenbin Kuang
Yongsoon Shin
Yeong-Shyung Chou
Yelin Ni
Yao Qiao
Daniel R. Merkel
Madhusudhan R. Pallaka
Xin Yang



U.S. DEPARTMENT OF ENERGY | Prepared for the U.S. Department of Energy under Contract DE-AC05-76RL01830

## DISCLAIMER



PACIFIC NORTHWEST NATIONAL LABORATORY
*operated by*
BATTELLE
*for the*
UNITED STATES DEPARTMENT OF ENERGY
*under Contract DE-AC05-76RL01830*

**Printed in the United States of America**

**Available to DOE and DOE contractors from the Office of Scientific and Technical Information,**
**P.O. Box 62, Oak Ridge, TN 37831-0062**
www.osti.gov
**ph: (865) 576-8401**
**fax: (865) 576-5728**
**email: reports@osti.gov**

**Available to the public from the National Technical Information Service**
**5301 Shawnee Rd., Alexandria, VA 22312**
**ph: (800) 553-NTIS (6847)**
**or (703) 605-6000**
**email: info@ntis.gov**
**Online ordering: http://www.ntis.gov**

PNNL-33736

# Gap Analysis on the Impacts of Hydrogen Addition to the North American Natural Gas Infrastructure Polyethylene Pipelines

July 2022

Kevin L. Simmons
Lisa Fring
Wenbin Kuang
Yongsoon Shin
Yeong-Shyung Chou
Yelin Ni
Yao Qiao
Daniel R. Merkel
Madhusudhan R. Pallaka
Xin Yang

Prepared for
the U.S. Department of Energy
under Contract DE-AC05-76RL01830

Pacific Northwest National Laboratory
Richland, Washington 99354

## List of Acronyms

| Acronym | Description |
|---|---|
| ASTM | American Society for Testing and Materials |
| BR | Brightness |
| CFR | Code of Federal Regulations |
| CNT | Circumferentially Notched Tensile |
| CO2 | Carbon Dioxide |
| CPENT | Cyclic Pennsylvania Edge Notch Tensile |
| CT | Computed Tomography |
| CTS | Copper Tubing Size |
| D | Diffusion Coefficient |
| DOC | Degree of Crystallinity |
| DSC | Differential Scanning Calorimetry |
| EN | European Standards |
| ESC | Environmental Stress Cracking |
| ESCR | Environmental Stress Cracking Resistance |
| FNCT | Full Notch Creep Test |
| GC | Gas Chromatography |
| GTI | Gas Technology Institute |
| H2 | Hydrogen |
| H2S | Hydrogen Sulfide |
| HDB | Hydrostatic Design Basis |
| HDPE | High Density Polyethylene |
| HDS | Hydrostatic Design Strength |
| HPHP | High Pressure Hydrogen Gas Permeation |
| IPS | Iron Pipe Size |
| ISO | International Organization for Standardization |
| LDPE | Low Density Polyethylene |
| LED | Light Emitting Diode |
| LLDPE | Linear Low Density Polyethylene |
| LTHS | Long Term Hydrostatic Strength |
| MDPE | Medium Density Polyethylene |
| MRS | Minimum Required Strength |
| N2 | Nitrogen |
| NG | Natural Gas |
| NOx | Nitrogen Oxides |
| O2 | Oxygen |
| OIT | Oxidative Induction Time |
| OITP | Oxidative Induction Temperature |
| P | Permeability Coefficient |
| PA | Polyamide |
| PDB | Pressure Design Basis |
| PE | Polyethylene |
| PENT | Pennsylvania Edge Notch Tensile |
| PHMSA | Pipeline and Hazardous Materials Safety Administration |
| PNNL | Pacific Northwest National Laboratory |
| PPDC | Plastic Pipe Database Collection Initiative |
| PPI | Plastic Pipe Institute |
| PSI | Pounds per Square Inch |
| RGB | Red, Blue and Green |
| RT | Room Temperature |
| S | Solubility Coefficient |
| SCG | Slow Crack Growth |

| | |
|---|---|
| SCGR | Slow Crack Growth Resistance |
| SDR | Standard Dimension Ratio |
| TDA | Thermal Desorption Analysis |
| TDA-GC | Thermal Desportion Analysis-Gas Chromatography |
| TN | Technical Note |
| TTS | Time-Temperature-Superposition |
| UHMWPE | Ultra High Molecular Weight Polyethylene |
| UV | Ultraviolet |
| VC | Volumetric Collection |
| WAXD | Wide-Angle X-ray Diffraction |

# Contents

Executive Summary ..... viii
1.0 Introduction ..... 1
1.1 Motivation ..... 1
1.2 Document Overview ..... 2
2.0 Materials and Design Background ..... 4
2.1 Polyethylene Materials Used in Natural Gas Pipelines ..... 4
2.2 Pipeline Design ..... 5
2.2.1 Pipe Structure ..... 5
2.2.2 Joints ..... 7
2.2.3 Defects ..... 9
2.3 Current State of the Existing Pipeline Network ..... 9
2.3.1 Pipeline Materials ..... 9
2.3.2 Causes of PE Pipeline Failures ..... 10
2.3.3 Failure Modes ..... 11
2.4 Lifetime Assessment Methods and Requirements ..... 14
2.5 Analysis and Key Take-Aways on Design and Lifetime Assessment for Pipelines of Blended Hydrogen and Natural Gas ..... 20
3.0 Considerations of Hydrogen Use in Polyethylene Pipeline Distribution Systems ..... 22
3.1 Mechanical Properties ..... 22
3.1.1 Quasi-Static Tensile Behavior ..... 22
3.1.2 Fatigue Tensile Behavior ..... 27
3.1.3 Creep Tensile Behavior ..... 28
3.2 Chemical and Physical Properties ..... 29
3.2.1 Degradation Induced Pipe Failure - Anti-Oxidant Depletion ..... 29
3.2.2 Physical Properties ..... 37
3.3 Hydrogen Losses Through Pipeline Permeation ..... 40
3.3.1 Mechanisms of Gas Permeation ..... 41
3.4 Analysis and Key Take-Aways on Chemical, Mechanical, Physical, and Transport Properties for Pipelines of Blended Hydrogen and Natural Gas ..... 49
4.0 Conclusions and Recommendations ..... 52
5.0 References ..... 53
6.0 Acknowledgements ..... 60

# Figures

Figure 1. Green hydrogen production, transmission, and distribution would be enabled by blending within the existing natural gas network. ..... 1

Figure 2. Map of the United States' natural gas distribution system ....2
Figure 3. Representative image of a butt fusion joint....7
Figure 4. Representative image of a saddle joint ....8
Figure 5. Representative image of a socket fusion joint ....8
Figure 6. Representative image of an electrofusion joint....8
Figure 7. Stress vs. failure time for PE pipes featured with ductile failure (Region I), brittle failure after slow crack growth (Region II), and material degradation (Region III) [30] ....12
Figure 8. An optical micrograph of the fracture face of a PE-2406 DuPont Aldyl A MDPE specimen after fatigue testing to failure[33] ....12
Figure 9. Scanning electron micrograph of the fibrillar structure in the craze zone of a notched polyethylene specimen experiencing slow crack growth[36]....13
Figure 10. Digital photos of (a) impingement and crack on the outer surface, (b) crack visible from the inner surface, and (c) micrograph of the fracture face of a DuPont Aldyl-A PE 2306 pipe[29]....13
Figure 11. Front and side views of a PE pipe showing ductile failure subjected to high pressure....14
Figure 12. Typical PENT test sample geometry for compression-molded PE materials. (Reprinted, with permission, from ASTM D F1473-18, *Standard Test Method for Notch Tensile Test to Measure the Resistance to Slow Crack Growth of Polyethylene Pipes and Resins*) ....16
Figure 13. Typical PENT test sample dimensions for PE pipes, (a) longitudinal specimen from 110-mm SDR 11 pipe with tensile axis parallel to the extrusion direction, (b) tensile axis perpendicular to the extrusion direction, (c) small pipe with outside diameter less than 25 mm (Reprinted, with permission, from ASTM D F1473-18, *Standard Test Method for Notch Tensile Test to Measure the Resistance to Slow Crack Growth of Polyethylene Pipes and Resins*) ....17
Figure 14. Schematic drawing shows the (A) razor blade notched sample, (B) sample holder, (C) multiple bent samples placed in specimen holder and inserted inside a glass tube filled with a thermally stable liquid for ESCR at 50°C or 100°C (Reprinted, with permission, from ASTM D F1693-21, Standard Test Method for Environmental Stress-Cracking of Ethylene Plastics). ....18
Figure 15. Effect of hydrogen (at 3 MPa pressure) on the uniaxial ultimate strength of HDPE at three temperatures. The ultimate strength reported corresponds to the first peak load; the entire load-displacement data was not provided in the paper. [15] ....23
Figure 16. Effect of hydrogen pressure on the uniaxial tensile properties of HDPE at room temperature: (a) ultimate strength (b) strain at the first peak load.[16, 42] ....24
Figure 17. Effect of hydrogen (3MPa pressure) on the Mode I dissipated and released energies (*i.e.* specific work of fracture) as a function of ligament area at room temperature[47]....25
Figure 18. Effect of interval time on the following failure behaviors of the MDPE pipe: (left) burst pressure; (right) maximum principal strain at failure[48]. Note that

the interval time means the time after taking the MDPE pipe with fully-soaked hydrogen from the hydrogen chamber. ....25
Figure 19. MDPE burst test specimens diplaying ductile failure; (left) hydrogen exposed specimen; (right) control specimen not exposed to hydrogen[48] ....26
Figure 20. Hardness (a) and elastic modulus (b) profiles of a representative pipe specimen as a function of location through the thickness (inner wall edge = 0 μm while outer wall edge = 10,000 μm) before exposure to hydrogen (black), immediately after exposure to 250 psi hydrogen for 72 h (red), and 14 days after the exposure (blue)[48] ....27
Figure 21. Effect of hydrogen on the stress-life curve (*i.e.*, maximum stress in applied cyclic stress vs. number of cycles) of MDPE obtained from Circumferentially Notched Tensile specimens[48] ....28
Figure 22. Effect of hydrogen on the evolution of logarithmic strain obtained from creep tests. Note that the results were constructed by using time-temperature-superposition principle[47, 52, 53](TTS). ....29
Figure 23. Oxidation onset is determined using (a) tangent method and (b) offset method....30
Figure 24. OIT at 210°C of harvested PE pipes used in Australia[67] and Algeria[67]....31
Figure 25. Rate of antioxidant depletion as a function of concentration based on Equation (5). ....33
Figure 26. OIT of PE80 MDPE and PE100 HDPE pipes after four years of exposure to pure hydrogen at 4 barg and 8°C. X-axis locations are slightly shifted for discernability[17]....35
Figure 27 (a)Degree of crystallinity as a function of hydrogen pressure for various PE types[46, 97, 99] and (b) MDPE pipe material[44] ....38
Figure 28 (a)Density as a function of hydrogen pressure for various PE types[46, 98, 99] and (b) MDPE material[44] ....38
Figure 29 Extent of destruction as a function of high-pressure hydrogen (left). Processed transmission light detection images (shown as a matrix) for PE disk specimens (right). X-ray CT image showing voids and damage on an LDPE disk specimen after 24-hour exposure to ....39
Figure 30. Hydrogen gas volume loss rate per year. (a) the temperature effect at 10 bar. (b) the pressure effect at 293 K[111] ....41
Figure 31. The diffusion mechanism of gas in the polymer, modified with permission from ref[112]....42
Figure 32. Effect of applied pressure on permeation testing at 30°C: (a) hydrogen permeation rate, (b) apparent permeability, (c) diffusivity, (d) solubility. Modified with permission from ref.[97] ....45
Figure 33. MDPE thermal desorption data.[46] (a) Desorption data, (b) pressure dependence of equilibrium hydrogen concentration and diffusion coefficient, and (c) crystallinity and density change post-decompression. ....46
Figure 34. Temperature dependence of hydrogen permeability of polymer materials, modified with permission from ref. [125] ....47
Figure 35. Effect of crystallinity in different PE polymers on hydrogen solubility in a high-pressure gas environment, reproduced with permission from ref.[46] ....47

Figure 36. Relative hydrogen permeability values for PE-based nanocomposite films prepared with different fillers. Modified with permission from ref.[127] ..... 48

## Tables

Table 1. Examples of ASTM D2513 pipe material designation codes, illustrating how current pipeline materials outperform historical ones ..... 4
Table 2. Sizing system example for polyethylene pipe ..... 5
Table 3. Percentages of PE failures by major causes[28] ..... 11
Table 4. Average temperature and annual precipitation of the service locations of tested PE pipes.[67, 68] ..... 31
Table 5. Pipeline gas specifications[88] ..... 35
Table 6. OIT profile of weld zone of PE pipes[81] ..... 36
Table 7. OIT of PE resins[81] ..... 37
Table 8. Estimated hydrogen and methane permeation rates in HDPE, MDPE, and PA11[107 108] ..... 40

# Executive Summary

The existing natural gas pipeline system is being considered as a means to distribute blends of clean hydrogen and natural gas as one component of clean hydrogen's role in enabling a future low-carbon energy system. With nearly three million miles of transmission and distribution lines in the United States, this national asset is uniquely situated as a transition strategy to assist in the decarbonization of the US economy. [1] This report reviews existing data on the effects of hydrogen on polyethylene (PE) natural gas pipeline materials and identifies gaps where additional investigation is required to fully assess deleterious impacts to the polyethylene pipes from exposure to hydrogen. This gap analysis will assist in determining the feasibility of blending hydrogen gas into existing natural gas pipelines.

Existing distribution natural gas pipelines are primarily made of medium density polyethylene (MDPE) and high density polyethylene (HDPE) materials that have proven reliable in this application for over fifty years. The resin formulations used for these pipes have evolved over the years to provide for stronger, more durable materials that are increasingly resistant to the major failure modes. The current regulations and standards require long-term strength testing to validate the life of the PE materials used for gas pipelines. Since time to failure is quite long for the new resin systems, an accelerated method to evaluate the lifetime of PE pipe when exposed to hydrogen under the actual pipeline operating conditions would support decision making.

Current lifetime validation methods center on long-term strength testing, but hydrogen's shorter-term mechanical, chemical, and physical effects on the PE must also be considered to fully understand compatibility. This report identifies the limited amount of existing data in each of these categories and lays out additional testing needs. Existing data is typically not traceable to the specific resin formulation of the pipe tested, and the specific impacts of varying resin formulations also need more investigation in terms of hydrogen effects. In addition, most of the test data in these categories were generated on the body of the pipe. More testing on hydrogen effects on heat fusion joint regions is needed.

The existing, short-term mechanical test data of hydrogen effects on PE materials is primarily focused on uniaxial stress states. Tensile testing in quasi-static loading in one report showed no significant effect from hydrogen at low pressures. Higher pressure testing indicated a slight decrease in tensile stress and strain with increasing pressure. It is not clear if this is a hydrogen effect or a pressure effect. In contrast, nanoindentation testing showed a decrease in the local modulus of a PE specimen exposed to hydrogen. Limited data on burst strength, mode I fracture energy, and fatigue tensile properties show no significant property reductions as a result of hydrogen exposure. Additional modes of fracture and fatigue test conditions, including fatigue specimens with a sharp notch, should be investigated. One study reported slightly lower deformation associated with hydrogen exposure in creep tensile testing, although this study was not purely experimental and multiple stress levels were not explored. Our review found no data on the effects of notches or defects on the creep behavior of PE in a hydrogen environment, an important consideration when evaluating the performance of pipe subjected to operational field conditions. Future testing should also evaluate multi-axial stress states in quasi-static, fatigue, and creep loading conditions.

In regards to material degradation, there is some oxidative induction time (OIT) data available that suggest hydrogen does not contribute to the depletion of antioxidants in PE pipe materials. The data available was limited to the body of the pipe and covered a limited range of environmental conditions. Additional OIT testing should be completed that encompasses the operating envelope of PE pipelines, including testing with hydrogen blends and impurities typical

to natural gas. OIT evaluation of heat fusion joint zones exposed to hydrogen both before and after joining is also needed.

Physical properties of PE material exposed to hydrogen, including degree of crystallinity and density, have been evaluated in some studies. Small changes (less than 5% decrease in crystallinity and less than 1% decrease in density) with hydrogen exposure were observed, and these changes may not be permanent. Investigation into the change in morphology of the crystallites with hydrogen exposure is needed to further understand these effects. PE exposed to hydrogen has also been characterized using light transmission and x-ray computed tomography. These techniques reveal that higher density PE materials exposed to pressurized hydrogen experience less damage compared to lower density PE materials. Coupling these characterization techniques with a technique to evaluate the crystallite morphology could provide greater understanding of material changes at the molecular level from hydrogen exposure and allow quantitative prediction of their effect on the mechanical performance and lifetime of pipes.

The permeability of hydrogen through the PE pipe wall is another key area of interest as this will affect leakage rates. This review identifies the existing hydrogen permeation data in PE but notes that consideration of material variables that could have an effect on permeation, such as crystallinity, degree of oxidation, and chain orientation in relation to thick wall pipe, is generally lacking. There is also a lack of permeability data on hydrogen/natural gas blends. Gathering this detailed data would allow the development of a predictive model of hydrogen permeation to aid in material design and selection.

# 1.0 Introduction

## 1.1 Motivation

In recent years, a focus on decarbonizing our economy has brought more attention to alternative energy sources such as hydrogen. Blending of clean hydrogen into natural gas pipelines is one pathway of interest to decarbonizing end uses in industry and buildings. Hydrogen is already used widely in the petrochemical industry, but broader use in other applications requires development of delivery infrastructure, such as pipeline materials.

One option under consideration for hydrogen delivery is the use of the existing natural gas distribution system.[2] Options under consideration include blending of hydrogen into natural gas such that the blends are consumed by traditional end uses of natural gas, or repurposing of the existing natural gas infrastructure to transport pure hydrogen. Blending beyond small concentrations is expected to require modifications to end-user appliances and to pipeline compression infrastructure and composition monitoring systems.[3, 4] Higher concentrations of hydrogen would also require higher pressures in the pipeline, increasing leakage and other concerns. Figure 1 illustrates how the natural gas system could be used to deliver hydrogen to consumers, a key step in increasing the use of hydrogen.

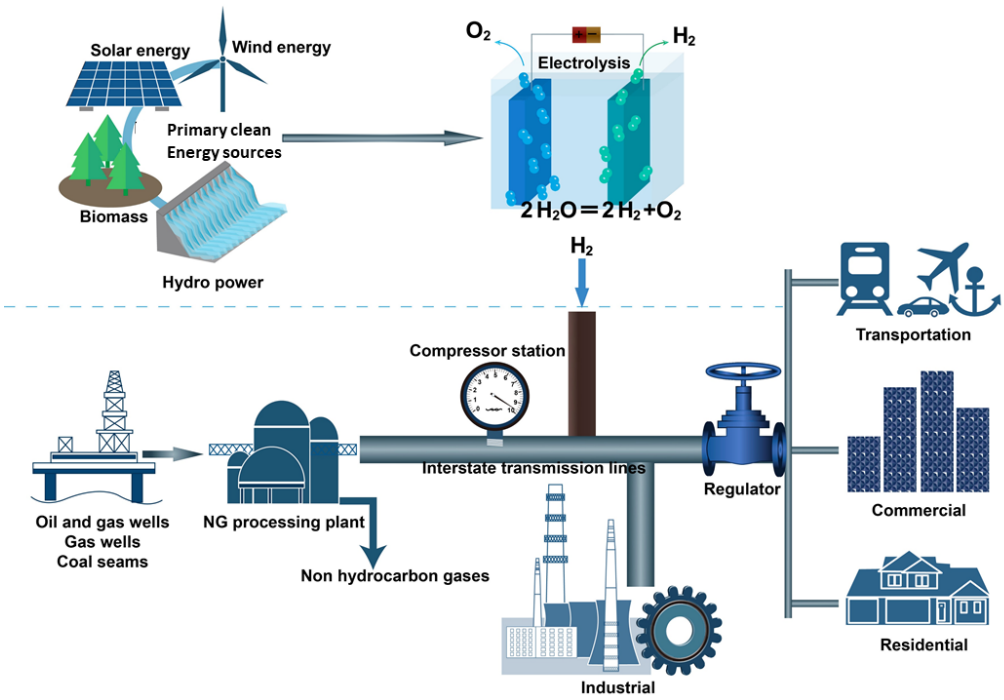


Figure 1. Existing natural gas network could potentially be used to transport clean hydrogen to variety of end uses.

Repurposing natural gas infrastructure for hydrogen delivery will require regional assessments of pipeline materials compatibility with hydrogen. The United States' natural gas distribution

system has approximately three million miles of pipeline, as shown in Figure 2.[1] While the system includes both metallic and polymeric piping, more than half of this piping is made of plastics, primarily polyethylene, including mains and service lines (laterals).[5]

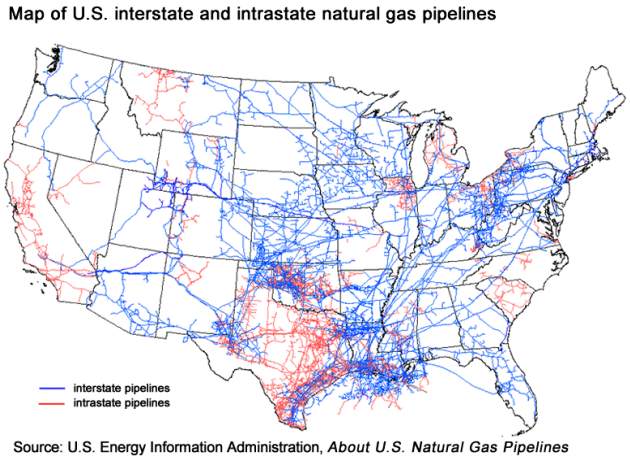


Figure 2. Map of the United States' natural gas distribution system

There has been extensive testing on the hydrogen compatibility of the metal materials found in the pipeline network.[6-9] However, the influence of hydrogen on polymeric pipeline materials has not been evaluated as rigorously. While some data shows that the effects of hydrogen on polymeric piping are negligible, the existing data is limited.[10-12] The existing data generally fail to consider resin formulation, joint regions, multi-axial stress states, effects of defects, and material degradation under actual operating conditions. Hence, enabling the vision in Figure 1 requires additional investigation into the interactions of both pure hydrogen and natural gas blended with hydrogen with polymeric piping.

## 1.2 Document Overview

This review has been conducted as part of the Pipeline Blending CRADA, a project within DOE's HyBlend initiative. HyBlend is an initiative that aims to address technical barriers to blending hydrogen in natural gas pipelines. The team is comprised of the National Renewable Energy Laboratory (NREL, the project lead, Technoeconomic analysis (TEA)), PNNL (polymer research lead), Sandia National Laboratories (SNL, metal research lead), Argonne National Laboratory (ANL, life cycle assessment) and more than 25 industrial partners. More detail about HyBlend and related research programs is available online at https://www.energy.gov/eere/fuelcells/hyblend-opportunities-hydrogen-blending-natural-gas-pipelines.

The objective of the review is to identify and assess the primary materials compatibility issues associated with this hydrogen blending concept, with a focus on the effects on medium density and high density polyethylene pipeline materials. Gaps in existing data and future opportunities for pipeline material evaluations and lifetime assessments will be identified.

This document begins by describing the current state of polyethylene natural gas pipelines, including their materials of construction, design basis, common defects, and failure modes. The standards and test methods currently used to assess pipeline lifetime are then presented. With this information as context, we will review these aspects for potential impacts of introducing hydrogen into the system.

We will then review the literature relative to the effects of hydrogen on polyethylene piping, including changes to both macroscopic properties such as tensile behavior and microscopic properties such as crystallinity. Permeation properties and hydrogen loss are briefly treated. This section concludes with analysis of the state of understanding of the effects of hydrogen on polyethylene that is relevant to pipeline lifetime, failure, and loss rates, along with a discussion of knowledge gaps.

The document concludes with a summary of what needs to be done to help decision-making about the feasibility of this approach, including the need for updated standards and additional data, and a prioritized set of information gaps.

# 2.0 Materials and Design Background

## 2.1 Polyethylene Materials Used in Natural Gas Pipelines

In the United States, polyethylene (PE) was introduced as a natural gas pipeline material in the 1950s, with the first installation of a high density polyethylene (HDPE) pipe occurring in 1959 in Kansas[13]. Touting lower installation and maintenance costs, utility companies started transitioning from metallic materials to polyethylene for distribution pipelines in the 1960s. It was the development of the extrusion process for fabricating PE pipe and the butt fusion process for joining pipe that helped enable the growth of this new material technology. Advancement of new resin formulations for higher performance and longer life has continued ever since. Higher performance in a pipeline application typically translates to *a higher pressure rating*, *resistance to oxidative degradation*, *resistance to slow crack growth*, and *resistance to rapid crack propagation*. Each decade saw new catalysts and resin formulations that improved upon these aspects.

By the 1970s, pipe with improved performance was introduced by resin manufacturers who had discovered how to broaden the molecular weight distribution and tailor the molecular branch length of PE[14]. Both medium density and high-density PE materials became available in this timeframe. While HDPE pipe offered a 25% higher pressure rating, medium density polyethylene (MDPE) was more resistant to cracking.

In this same timeframe, ASTM D2513, *Standard Specification for Thermoplastic Gas Pressure Piping Systems*, was released to define the requirements for these materials. While ASTM D2513 originally covered several thermoplastic materials, it has since been revised to cover only PE materials. ASTM D2513 introduced a designation code for pipeline materials that consists of an abbreviation for the type of polymer (PE) followed by four digits that describe the material's key properties: its density (first digit), its resistance to slow crack growth (second digit, coded 4, 5, 6, or 7 for 10, 30, 100, or 500 hours, respectively), and its hydrostatic design strength (third and fourth digit). For the latter two properties, larger numbers correspond to better performance. Table 1 shows examples of designation codes for both current and historical PE formulations.

Table 1. Examples of ASTM D2513 pipe material designation codes, illustrating how current pipeline materials outperform historical ones

| Pipe Material Designation Code | First Digit (Density, g/cc) | Second Digit (Minimum PENT hrs.) | Third and Fourth Digit (Maximum HDS, psi) |
|---|---|---|---|
| PE2708 (Current) | >0.925-0.940 | 500 | 800 |
| PE2406 (Historical) | >0.925-0.940 | 10 | 625 |
| PE4710 (Current) | >0.947-0.955 | 500 | 1000 |
| PE4608(Historical) | >0.947-0.955 | 100 | 800 |

ASTM D2513 has been revised several times to increase and add new requirements for piping materials. Resin manufacturers have developed unique formulations to meet the requirements of the specification, and multiple formulations fall under each code designation.

Pipeline materials are sometimes denoted PE80 and PE100; these designations originate from the European and International standards for pipeline materials, mainly EN 1555 and ISO 12162. These designations are based on the long-term strength of the material in terms of the Minimum Required Strength (MRS) of a pipe subjected to a long-term pressure test. The MRS of PE80 is 8 MPa, and the MRS of PE100 is 10 MPa.

Table 1 illustrates the significant improvement in slow crack growth resistance (demonstrated through the Pennsylvania Edge Notch Tensile (PENT) test requirement) and in hydrostatic design strength (HDS) realized with the newer materials. Modern PE piping materials have service lifetimes of at least 50 years, and the actual test results on the modern PE formulations typically far exceed the ASTM defined requirements. For example, one particular formulation of PE2708 reports PENT results of 15,000 hours.[15] This is 10,000 times higher than the performance of the very first generation of PE materials for pipelines.[16]

Some newer HDPE resin systems utilize a bimodal molecular weight distribution, where the presence of both short and long molecular chain lengths provides for a combination of excellent mechanical properties and processability. One relatively recent development uses a high level of short chain branching on longer chains to drive the branches into the amorphous region of the material, forming more tie molecules between the crystalline regions.[14] This approach greatly increases polymer strength and resistance to slow crack growth.

## 2.2 Pipeline Design

In the United States, 49 Code of Federal Regulations (CFR) Part 192 is the governing document for safety standards for natural gas pipelines and defines the design, installation, maintenance, and repair requirements. Note that the scope of this regulation includes gases other than natural gas, as the title states: “Transportation of Natural and Other Gas by Pipeline: Minimum Federal Safety Standards”.

This section outlines the design requirements and allowable operating conditions for the pipeline.

### 2.2.1 Pipe Structure

This section provides background information on how the operating conditions of the pipeline are determined and substantiated. Testing at the operating conditions will be discussed in several later sections of this review.

When referring to nominal pipe size, polyethylene pipe typically utilizes Iron Pipe Size (IPS) or Copper Tubing Size (CTS) identification to describe the pipe diameter. The Standard Dimension Ratio (SDR) is also commonly referenced for dimensioning purposes. The SDR is the ratio of the average outside diameter to the minimum wall thickness. ASTM D2513 further limits the eccentricity to less than 12%. An example of this sizing system is shown in Table 2.

Table 2. Sizing system example for polyethylene pipe

| Nominal Size (in.) | Outside Diameter (in.) | Minimum Wall Thickness (in.) | SDR |
|---|---|---|---|
| ½” CTS | 0.625 | 0.090 | 7 |

| | | | |
|---|---|---|---|
| ½” IPS | 0.840 | 0.090 | 9.3 |
| 1” CTS | 1.125 | 0.099 | 11 |
| 1” IPS | 1.315 | 0.119 | 11 |
| 2” IPS | 2.375 | 0.216 | 11 |

The code (49 CFR 192) states, “Pipe must be designed with sufficient wall thickness, or must be installed with adequate protection, to withstand anticipated external pressures and loads that will be imposed on the pipe after installation.” The design pressure for polyethylene distribution systems is not to exceed a gauge pressure of 100 psig, with an allowable exception of 125 psig for certain pipe materials with specific manufacturing dates and sizes. The design pressure (*P*) is calculated as follows:

$$P = 2S\left(\frac{t}{D-t}\right) \times DF \quad (1)$$

or, since *SDR* = *D/t,*

$$P = \frac{2S}{(SDR-1)} \times DF \quad (2)$$

where:

*P* = design pressure, gage,
*S* = hydrostatic design basis (HDB),
*t* = specified wall thickness,
*D* = specified outer diameter,
*SDR* = standard dimension ratio, and
*DF* = design factor (guidance is provided in the CFR for this value).

The hydrostatic design basis (HDB), or *S* in the equations above, is a material property obtained from long-term hydrostatic strength testing. The HDB for piping materials must be substantiated under specific temperature and pressure conditions, as defined in 49 CFR 192 and ASTM D2513. Approval for each resin formulation is documented by the Plastic Pipe Institute (PPI) in the TR-4 document, “PPI Listing of Hydrostatic Design Basis (HDB), Hydrostatic Design Stress (HDS), Strength Design Basis (SDB), Pressure Design Basis (PDB) and Minimum Required Strength (MRS) Rating For Thermoplastic Piping Materials or Pipe.” Appendix XI of ASTM D2513 states that the test medium for the HDB test should be natural gas or simulated natural gas. Water may be used as the test medium if the previous testing demonstrates that water and gas give the same test results for that particular type of PE.

The minimum allowable operating temperature for the plastic pipe is -20°F, with an exception up to -40°F only if the pipe has a temperature rating by the manufacturer. The maximum allowable operating temperature is the temperature at which the HDB used in the design pressure calculation was determined.

### 2.2.2 Joints

A joint is a point where two pieces of pipe, or a piece of a pipe and a fitting, are joined. In accordance with 49 CFR 192, joining procedures must be documented in a qualified procedure that has been proven to produce strong, gastight joints. Personnel performing joining operations must also be qualified through training and test. Plastic pipe may be joined by solvent cement, adhesive, mechanical or heat fusion methods. The use of threaded or miter joints is not permissible. For PE-type plastic pipe, heat fusion joints and compression-type mechanical joints are used. ASTM D2513, referenced by the CFR, further outlines requirements for joints.

Within the category of heat fusion joints, there are several subcategories including butt fusion, socket fusion, electrofusion, and saddle fusion. The principle behind these methods is the same. The surfaces to be joined are heated to a specified temperature and melt fused together by the application of a specified force. The key process parameters are cleanliness, temperature profile, and pressure. Heat fusion of dissimilar PE resins has historically been performed, and data suggests that it results in acceptable joints. The Plastic Pipe Institute issued Technical Note (TN) 13 in 2007 with guidelines for heat fusion joining of different PE pipe materials[17] (e.g. Dow MDPE to Chevron Phillips MDPE or Chevron Phillips MDPE to INEOS HDPE).

Butt fusion is one of the most frequently used methods to join pipe lengths. The two ends to be joined are cleaned and aligned so that the end faces are parallel, and the ends are heated, typically by the use of a hot plate. The two ends are then quickly pressed together and held under a specific pressure as they cool. The use of a clamping tool assists in controlling this process. A butt fusion joint is shown in Figure 3.

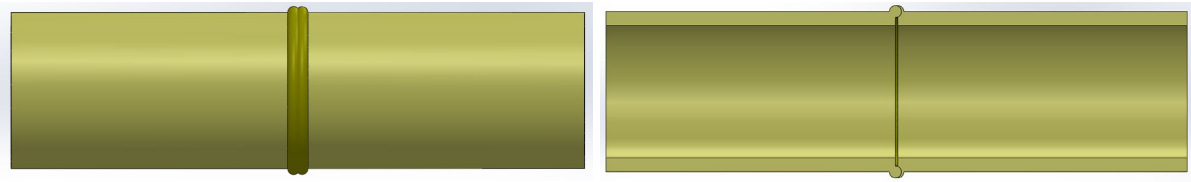

Figure 3. Representative image of a butt fusion joint

Saddle fusion and socket fusion operate on the same heat fusion principles as butt fusion but differ geometrically.

- In saddle fusion, a sidewall fitting is fused onto the side of the main pipe in a transverse orientation to the main pipe. Concave and convex heater plates are used to apply heat to the outside diameter of the main pipe and the inner surface of the fitting. A saddle fusion joint is illustrated in Figure 4.
- Socket fusion involves joining a pipe to a parallel, in-line fitting. The external surface of the pipe and the internal surface of the fitting are heated, and then the pipe is inserted in the socket and held during cooling. Socket fusion requires less pressure than butt fusion and is commonly used on pipes 4 inches in diameter and less. A socket fusion joint is shown in Figure 5.

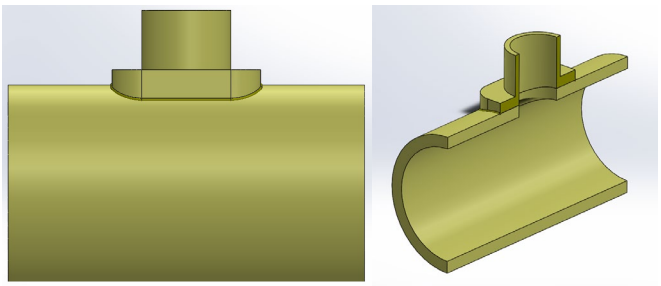

Figure 4. Representative image of a saddle joint

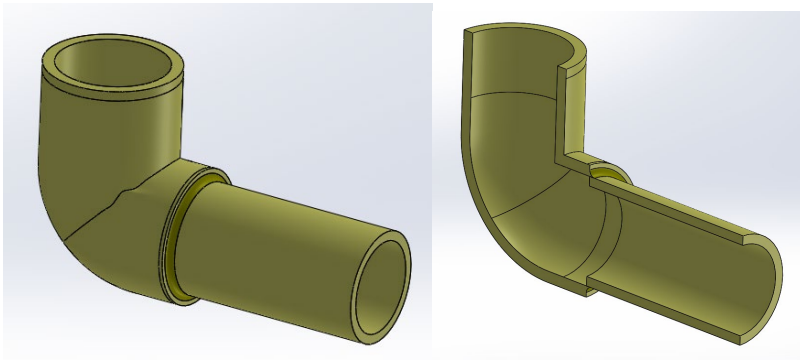

Figure 5. Representative image of a socket fusion joint

Electrofusion differs from the methods described above in that a resistive wire built into the fitting is used to provide the heat for joining. Electric current is applied to the wire, and the wire heats up and melts the outside diameter of the pipe and the inside diameter of the fitting. An electrofusion joint is shown in Figure 6.

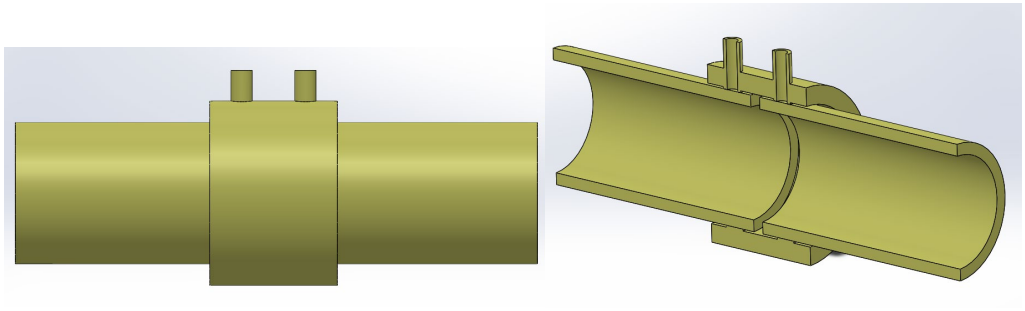

Figure 6. Representative image of an electrofusion joint

The fusion area, or weld zone, and the adjacent heat-affected zone typically differ in properties from the base pipe. These changes are attributed to changes in microstructure that occur during the heating and cooling involved in the fusion process. Polyethylene is a semi-crystalline polymer, having both amorphous and crystalline regions. The growth of the crystalline region is dependent on the temperature gradient and cooling rate experienced by the material. Multiple regions of distinct microstructural differences due to temperature gradients during fusion have

been found in the weld zone.[18] A high level of process control is required during heat fusion joining to control these microstructural changes and ensure that the strength requirements of the joint are consistently met.

Within the category of mechanical joints, there are several subcategories including hydraulic compression couplings, bolted and screwed compression couplings, stab type compression couplings, and interior seal couplings.[19] Even within the sub-categories, designs and materials used vary widely. Most mechanical joints employ an O-ring seal or gasket, a gripping device, and a stiffener to provide sealing and prevent pipe movement. Common materials used in mechanical couplings include polyethylene, polyamide, polyacetal, nitrile, stainless steel, and zinc plated carbon steel. ASTM F1924, “Standard Specification for Plastic Mechanical Fittings for Use on Outside Diameter Controlled Polyethylene Gas Distribution Pipe and Tubing,” further defines requirements and test methods for the qualification of mechanical fittings.

### 2.2.3 Defects

Defects can occur in polyethylene pipes from the pipe manufacturing process or during pipe transportation and installation. Types of defects from the manufacturing process may include contamination, inclusions, cavities, and melt irregularities. 49 CFR Part 192.59 states that plastic pipe must be free of visible defects to be qualified for use. The regulations and standards do not state if the visual inspection is to be performed with the aided or unaided eye. Quality control procedures that include visual inspection at the pipe manufacturer typically catch most defects from the manufacturing process prior to installation. While research has been ongoing, equipment-aided nondestructive inspection techniques, such as ultrasonic or radiographic, have not been proven yet for the inspection of plastic pipe.

During transportation and installation, common defect types include cuts, scrapes, gouges, and punctures. These are most common on the outer surface of the pipe. Because these pipes are buried underground, rock impingement is a very common defect cause. 49 CFR Part 192.311 states that each imperfection or damage that would impair the serviceability of plastic pipe must be repaired or removed. Part 192.605 requires each operator to have a manual of written procedures for maintenance and repair of the pipeline. Typical guidelines state that damage should not exceed 10% of the minimum wall thickness required for the pipeline’s operating pressure.[17] Pipes with defects that exceed that guideline are typically replaced by extracting the damaged section and fusing a new piece of pipe into place.

## 2.3 Current State of the Existing Pipeline Network

### 2.3.1 Pipeline Materials

Distribution pipelines represent the greatest pipeline mileage in the United States. In 2020, the distribution network consisted of over 1.5 million miles of plastic piping. Over 98% of this piping is made from PE plastic material.[20] While new PE resin formulations are constantly being developed and provide higher-performing pipes, historical resin systems are still prevalent in the pipeline network. The Pipeline and Hazardous Materials Safety Administration (PHMSA) collects data yearly from operators on total pipeline mileage, mileage by material, and installation dates. The “mileage by material” report is broken down into polymer types, but it does not specify the exact ASTM D2513 designation for the PE piping. The data collected on installation dates are not broken down by material type, so the data on the age of PE piping

specifically in the network is not available through these reports. Information provided by some operators suggests PE piping dating back to the 1970s is still present in the network.

The PHMSA also collects pipeline incident data, and this information is tracked by the exact material type involved in the incident. A review of this data collected from 2010 through 2021 shows the presence of PE2306 and Aldyl A materials with installation dates of 1970 and 1972[21]. Aldyl A is a specific manufacturer's designation for pipes that were made from a PE resin introduced to the market in 1965. The original version of this resin formulation was called Alathon 5040. Several resin formulation changes were made after its introduction. Pipes made from the formulation introduced in 1970, Alathon 5043, and manufactured between 1970 and 1972 experienced a manufacturing issue associated with high extrusion temperatures. This resulted in low ductility at the inner wall that, when coupled with the low resistance to slow crack growth associated with earlier resin systems, led to premature, brittle cracking. A new Aldyl A resin system, Alathon 5046, was introduced in 1983 that had improved resistance to slow crack growth. Efforts started in the early 2000s to replace Aldyl A pipes manufactured before 1983 prompted by a National Transportation Safety Board (NTSB) report in 1998 warning of the dangers of brittle-like cracking through slow crack growth for all pipes manufactured through the early 1980s.[22]

Because the "date of installation" based on material type is not tracked by all operators or PHMSA, it is difficult to determine exactly what vintage resins are still in use in the pipeline network, but there is evidence that some pipes in service date back to the 1970s.

### 2.3.2 Causes of PE Pipeline Failures

Two main data sources of PE gas distribution pipeline failure cases are publicly available from (1) PHMSA[20, 21] and (2) Plastic Pipe Database Collection Initiative (PPDC).[23]

PHMSA requires reporting of severe incidents resulting in death, in-patient hospitalization, $122,000 or more property damage, etc, as stated in 49 CFR Part 192. A statistical summary of incidents reported to PHMSA from 1984 to 2006 has been documented by the Gas Technology Institute (GTI) after re-examination of the contents[24]. Failed pipe samples during 2006 to 2009 were re-analyzed by GTI and included in the same report.[24] The GTI report concluded that the most significant failure mode for PE pipes was slow crack growth (SCG). Until January of 2022, 1293 incidents were listed in PHMSA "Gas Distribution Annual Data – 2010 to present" spreadsheet[20, 21], among which 398 cases (31%) were polyethylene pipes. Excavation is the main cause of PE pipe failures, accounting for 212 out of 398 (53%). Of the 49 cases of PE pipe failures that were attributed to material failure (~12% of the total of 398), failures occurred at the pipe body (14/49, 29%), joints (32/49, 65%), or other parts (3/49, 6%). Without access to detailed reports of each incident, the root cause of PE pipe failure was unknown. From the brief narratives included in PHMSA data entries[20, 21], causes appear to be qualitatively consistent with what has been identified in the GTI report[24], namely lack of fusion, fitting failures, rock impingement, bending, and internal pressure, which further lead to slit SCG or rupture.

The PPDC database is composed of data voluntarily submitted by industrial operators, with a particular interest in the plastic pipe system failures and leaks unrelated to excavation damage. Statistical summaries of collected data are updated online.[23] As of May 2018, 119 corporations that account for 76% of the total mileage of main in the U.S. and 86% of the total number of services are considered as active submitters to the database. Despite broad participation, the PPDC database is subject to the inherent limitation "pertaining to the accuracy that comes with volunteer surveillance data". Specifically, no independent analysis is performed to verify the

accuracy or to study further the failures or leaks reported as “cause unknown,” which accounted for 15-50% of cases. Also, the lack of standardized reporting procedures has been a concern. In addition, the total number of cases is not shared, and consequences such as property damage and gas loss are not evaluated. When causes are considered known, the primary causes cited for PE pipe, fitting, and joint failures are installation error and material defect. Percentages of major causes listed in the latest status report published in June 2021 are given in Table 3.

Table 3. Percentages of PE failures by major causes[23]

| | Failures in Components | | | Overall |
|---|---|---|---|---|
| Cause | Pipe | Fitting | Joint | |
| Installation Error | 6.2% | 26.9% | 56.0% | 21.6% |
| Material Defect | 12.3% | 15.8% | 10.4% | 13.7% |
| Point Loading | 9.8% | 1.9% | 2.2% | 5.3% |
| Other | 9.6% | 12.6% | 4.4% | 10.3% |
| Unknown | 48.4% | 24.0% | 17.7% | 33.5% |

Comparing between components, 31.2% of PE failures were in the pipe body (close to 29% in PHMSA database[21]), 53.9% in fittings, 11.7% in joints, and 3.2% unknown. As fittings and joints are convoluted in PHMSA reporting, the total percentage of fitting and joints being 65.6% is also comparable to the PHMSA data (65%).

### 2.3.3 Failure Modes

Further identifying phenomenological material failures into modes or mechanisms requires lab testing of samples that failed in field service. Among the 49 incidents reported to PHMSA[21] regarding PE distribution pipe failures since 2010, seven entries mentioned modes of failure in the brief narratives, specifically,

- “stress-induced crack near joint,”
- “slow crack growth as a result of multiple stress applied to the fitting,”
- “slow crack growth resulting from pipe deflection and non-fusion,”
- “thermal oxidation resulting in axial slit crack,”
- “fracture propagated by slow crack growth driven by the system pressure,”
- “excessive bending strain,” or
- “external point load from rock impingement”[21]

These descriptions are all consistent with features observed in slow crack growth (SCG), which is the major cause of PE distribution pipe failures.[24] Ductile failure is less frequently observed but also accounted for 1% of PE gas pipe failures.[24] Schematic representation of these two mechanical failure modes is given in Figure 7.[25-27] Ductile failure happens at high stress (Region I), whereas brittle failure happens after stable crack growth (Region II). At longer service time, material degradation (Region III) such as oxidation reduces the service life of PE due to the increased frequency of brittle failure.

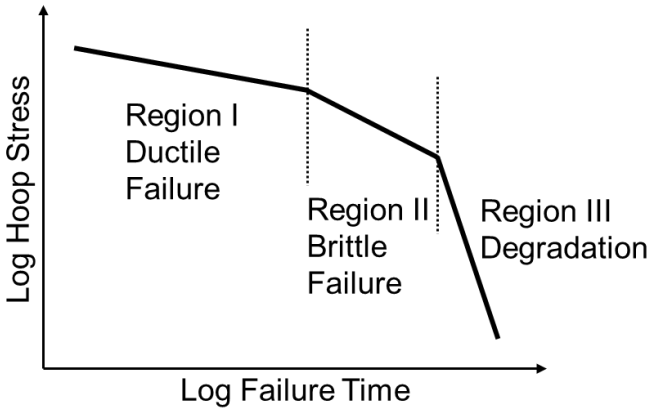


Figure 7. Stress vs. failure time for PE pipes featured with ductile failure (Region I), brittle failure after slow crack growth (Region II), and material degradation (Region III) [25]

Slow crack growth refers to stepwise or quasi-continuous propagation of the craze zone at low loads below yield, leading to brittle fractures with small deformation. Modes of stepwise vs. quasi-continuous growth depend on loading condition and temperature. In the case of stepwise growth, the fracture face exhibits striation marks as shown in Figure 8.[28]

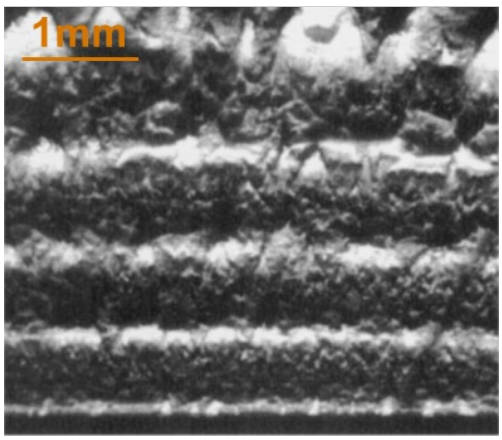


Figure 8. An optical micrograph of the fracture face of a PE-2406 DuPont Aldyl A MDPE specimen after fatigue testing to failure[28]

The initiation mechanism for SCG can be stress concentration caused by manufacturing defects, contaminants, cavities, stress risers, etc. A typical case is SCG initiated by a notch, where the craze zone is filled with fibrillar structures as shown in Figure 9.[29-31] Accompanied by crack growth, interlamellar “tie chains” experience disentanglement and scissions. The striation pattern shown in Figure 9 consists of remnants of broken fibrils. Resistance to SCG is related to polymer microstructures , molecular weight, and chain branching.[31]

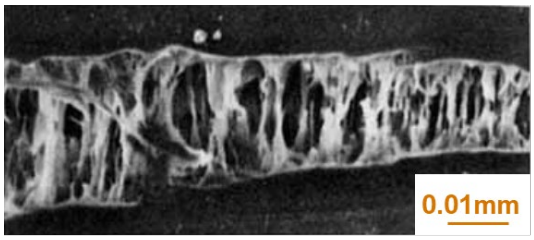


Figure 9. Scanning electron micrograph of the fibrillar structure in the craze zone of a notched polyethylene specimen experiencing slow crack growth[31]

Figure 10 presents photos of a DuPont Aldyl-A PE 2306 pipe in service from 1984 to 2008 as a typical case of SCG failure. After material and mechanical properties were measured in the laboratory, failure analysts concluded that the failure originated from the impingement observed in the outer wall of the pipe (Figure 10a). From that point, the crack grew along two longitudinal directions as well as through the wall thickness and reached the inside of the wall (Figure 10b).[24] Montaged microscopic photos (Figure 10c) of the fracture face showed two striation zones, indicating stepwise growth of the crack.

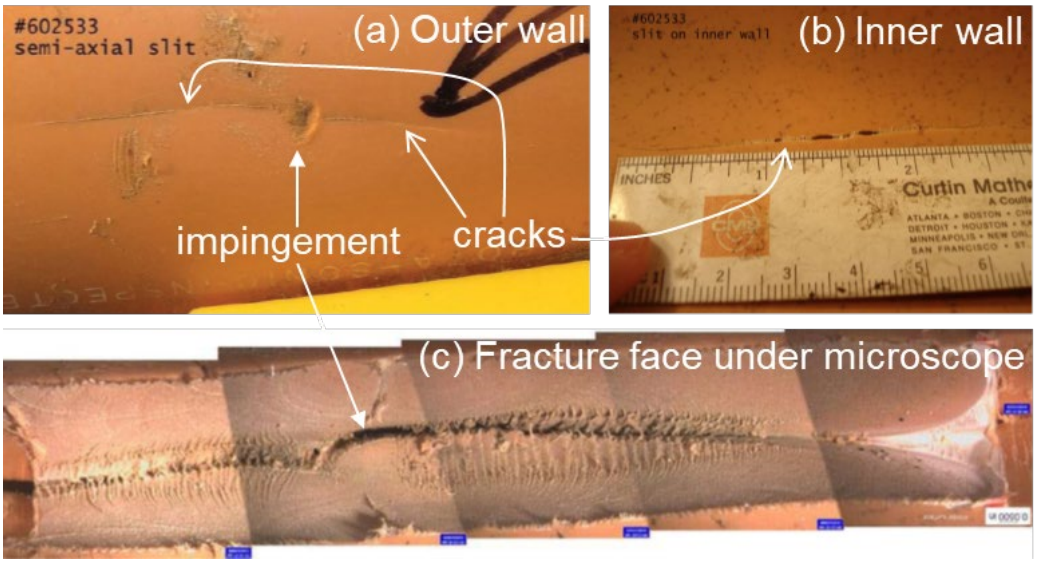


Figure 10. Digital photos of (a) impingement and crack on the outer surface, (b) crack visible from the inner surface, and (c) micrograph of the fracture face of a DuPont Aldyl-A PE 2306 pipe[24]

Slow crack growth is the dominant, but not only, mechanism of failure. Ductile failure accounts for only 1% of failures and is typically caused by accidental overpressurization. Unlike SCG, ductile failure happens at a time scale of minutes after a high internal pressure is applied (>400 psig)[24], during which material experiences large deformation, yielding, ballooning, and wall thinning, as shown in Figure 11.

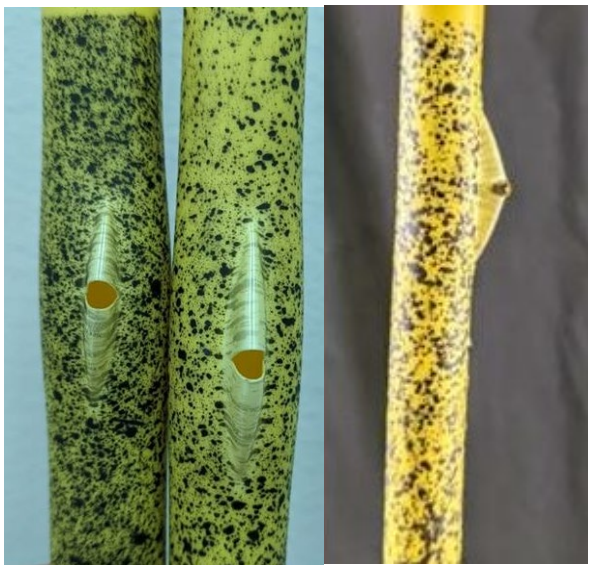

Figure 11. Front and side views of a PE pipe showing ductile failure subjected to high pressure

## 2.4 Lifetime Assessment Methods and Requirements

The previous subsections have reviewed the materials of construction, design considerations, and failure modes for PE pipeline used in natural gas infrastructure. A key goal of the current project is to evaluate impact of hydrogen blended into natural gas on pipeline lifetime. Hence, this section reviews current lifetime assessment standards for PE materials, including test methods, requirements, and limitations. In this section, only slow crack growth (SCG) resistance, environmental stress-cracking resistance (ESCR), and hydrostatic design stress (HDS) are reviewed and discussed.

Currently, six ASTM standards address the lifetime assessment of PE materials:

- *ASTM D2513-19: Standard Specification for Polyethylene (PE) Gas Pressure Pipe, Tubing, and Fittings*
- *ASTM D3350-14: Standard Specification for Polyethylene Plastics Pipe and Fittings Materials*
- *ASTM F1473-18: Standard Test Method for Notch Tensile Test to Measure the Resistance to Slow Crack Growth of Polyethylene Pipes and Resins*
- *ASTM D1693-21: Standard Test Method for Environmental Stress-Cracking of Ethylene Plastics*
- *ASTM D2837-13: Standard Test Method for Obtaining Hydrostatic Design Basis for Thermoplastic Pipe Materials or Pressure Design Basis for Thermoplastic Pipe Products*
- *ASTM D1598-15a: Standard Test Method for Time-to-Failure of Plastic Pipe Under Constant Internal Pressure*

Two of these standards (ASTM D2513 and D3350) define the standard specifications for PE pipes and fitting materials. The other four standards (ASTM F1473, D1598, D1693, and D2837)

detail the actual test methods to measure lifetime-related mechanical properties and materials requirements. The six standards are reviewed below with emphasis on test methods and requirements rather than specifications or code designations.

*ASTM D2513-19: Standard Specification for Polyethylene (PE) Gas Pressure Pipe, Tubing, and Fittings*

This standard specification covers requirements and test methods for material dimensions and tolerances, hydrostatic burst strength, hydrostatic design basis, chemical resistance, slow crack growth, and rapid crack resistance of polyethylene pipe, tubing, and fittings intended for natural gas transmission and distribution, either for direct burial or re-liner applications. This standard lists the materials' requirements for polyethylene compounds suitable for manufacturing pipe and fittings under this specification code. Only two types of PE are listed in this standard: PE2708 and PE4710. Other pipe materials such as PE 2306, PE 2406, PE 2606, PE 3306, PE 3406, PE 3408, PE 3608, PE 3710, and PE 4608 are eliminated in D2513 to reflect the current state of the art in PE piping specified for applications within the scope of this specification. They can still be used for gas transmission or distribution. D2513 lists requirements for resistance to slow crack growth (SCG performed by ASTM F1473, described below) for both PE2708 and PE 4710, i.e., a minimum failure time of 500 h in an accelerated test condition of 80°C and 2.4 MPa in air using molded PE plaque samples with a sharp notch. The specification also requires HDB to be substantiated for linear pipe up to 50 years (D2837 section 5.7) of 1250 psi for PE2708 and 1600 psi for PE4710 for samples tested at 23°C.

*ASTM D3350-14: Standard Specification for Polyethylene Plastics Pipe and Fittings Materials*

This specification provides a classification system for polyethylene plastic pipe and fittings materials. It does not provide specific engineering data for design purposes, specify manufacturing tolerances, or determine suitability for use for a specific application. D3350 classifies polyethylene plastics pipe and fittings materials into seven categories: density, melt index, flexural modulus, tensile strength at yield, slow crack growth resistance, hydrostatic design basis, and color and UV stabilizer. Two methods are listed to specify the slow crack growth resistance of PE pipes and fittings in D3350: environmental stress-cracking following method ASTM D1693 and slow crack growth with the PENT method following method ASTM D1473, both of which are described in the following sections.

*ASTM F1473-18: Standard Test Method for Notch Tensile Test to Measure the Resistance to Slow Crack Growth of Polyethylene Pipes and Resins*

This standard test method, developed by Lu and Brown in 1992[32], is also called the Pennsylvania Edge Notch Test (PENT). It measures the resistance to slow crack growth of polyethylene pipe and resins with specified notches. The purpose of the notch is to introduce a triaxial stress state at the notch tip to ensure a slow and brittle fracture process with little macroscopic plastic deformation. The load is chosen such that the stress at the notch tip (ligament stress = 2.4 MPa) is well below the material's yield stress. The outcome of this test is the time to failure or the time it takes for the two halves of the specimen to fully separate or reach a separation of 0.5 inches, whichever comes first. The resistance to SCG fracture is then related to the PENT failure time. The test is typically conducted at 80°C to accelerate the brittle fracture process. It may also be done at lower temperatures (<80°C) with low enough stresses to preclude ductile failure and eventually induce brittle failure.

In general, polyethylene will ultimately fail in a brittle manner by slow crack growth at 80°C if the stress is below 2.4 MPa. The method utilizes compression-molded PE resins where specific temperature and time ranges are required in molding the resins per ASTM F1473 and D4703. The compression-molded plaque is machined to desired thickness (ranging from 4 mm to 20 mm) and rectangular shape and notched using a razor blade of a set thickness at the specified speed. The main notch depth used is dependent on sample thickness, which is listed in ASTM F1473, while the depth of two side notches is fixed at 1.0 ± 0.10 mm. Figure 12 shows a typical compression molded sample of 10 mm x 25 mm x 50 mm with a main notch depth of 3.5 mm and side notches of 1.0 mm on both edges. For PE pipe and fitting materials, the average of failure PENT time (in hours) of two test samples shall meet the specification as listed in ASTM D3350. Only four numbered codes are given in the standard (D3350) for use as the second digit in the material designator; codes 4, 5, 6, and 7 have corresponding minimum PENT failure time (hours) at 80°C and 2.4 MPa of 10, 30, 100, and 500 hours, respectively.

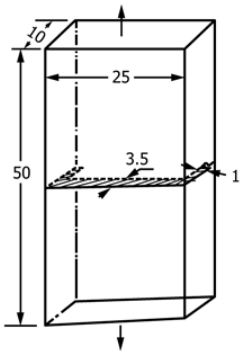


Figure 12. Typical PENT test sample geometry for compression-molded PE materials. (Reprinted, with permission, from ASTM D F1473-18, *Standard Test Method for Notch Tensile Test to Measure the Resistance to Slow Crack Growth of Polyethylene Pipes and Resins*)

The method may also be applied to extruded pipes and tubing, which is non-mandatory. Typical examples of the test sample are illustrated in Figures 13(a), 13(b), and 13(c) for tensile axis direction parallel to pipe extruded direction, tensile axis direction perpendicular to extruded direction, and pipes with outside diameter less than 25 mm, respectively. For extruded pipes, the notch direction is an important factor because the long polyethylene molecules tend to align with the pipe's extrusion direction. This leads to better apparent performance for notching perpendicular to the extrusion direction (Figure 13(a)) than notching parallel to the extrusion direction (Figure 13(b)). In addition to notch direction, other test parameters can also affect the PENT failure time: temperature, stress, notch depth, and specimen geometry. In general, increasing temperature, stress, and notch depth decrease failure time. Pigments can also impact the results (color or carbon black), as can the carrier resin for the pigment, and dispersion and distribution of pigment. Thus, in reporting the test time or time to failure, all the test conditions shall be specified.

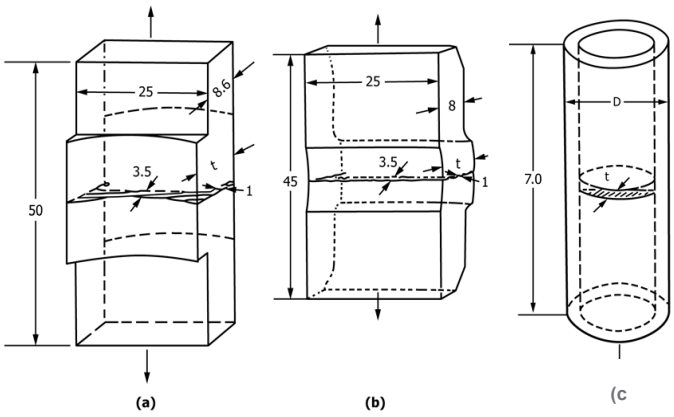


Figure 13. Typical PENT test sample dimensions for PE pipes, (a) longitudinal specimen from 110-mm SDR 11 pipe with tensile axis parallel to the extrusion direction, (b) tensile axis perpendicular to the extrusion direction, (c) small pipe with outside diameter less than 25 mm (Reprinted, with permission, from ASTM D F1473-18, *Standard Test Method for Notch Tensile Test to Measure the Resistance to Slow Crack Growth of Polyethylene Pipes and Resins*)

ASTM F1473 offers a much faster method for measuring SCG than methods using un-notched specimens. It shows good intra-laboratory ( ±16%) and inter-laboratory (±26%) precision when performed using a precision notching machine and a sharp razor blade at the specified conditions. The details of apparatus, sample preparations, conditioning, precautions, and procedures can be found in F1473.

*ASTM D1693-21: Standard Test Method for Environmental Stress-Cracking of Ethylene Plastics*

In addition to SCG, environmental stress cracking can occur in PE pipes installed for natural gas transmission and distribution because the majority of these pipes are buried one to three feet underground, where they are exposed to loads and to moisture. ESCR can lead to premature failure. D1693 describes a standard test to quantify ESCR by using bent specimens with a controlled notch on one surface that is then exposed to a surface-active agent. Rectangular plate samples are typically used with a length of 38 ± 2.5 mm, width of 13 ± 0.8 mm, and varying thickness depending on the test temperature of either 50°C or 100°C (see Table 1 in D1693). The test samples are first conditioned in the appropriate liquid at a specified temperature for 40 to 90 h before being pressed with a razor blade to introduce a controlled imperfection (Figure 14A). The notched samples are then bent with a bending clamp assembly and placed inside a specimen holder (Figure 14B). Ten specimens are then stacked in the specimen holder and placed inside a glass pipe filled with a thermally stable liquid (Figure 14C) such as nonylphenoxy poly(ethyleneoxy) ethanol (Igepal CO-630) and in a constant temperature bath. The samples are then periodically examined visually to see if a crack

develops. Any crack visible to a normal observer shall be interpreted as a failure of that specimen, and the time to failure is recorded (in hours).

In general, the crack develops from the controlled imperfection (notch) and runs perpendicularly to the outer edges of the bent section, which is under stress and directly observable. The cracks need not extend entirely through the specimen to constitute failure. Cracks may develop under the polymer surface, manifesting themselves as depressions on the surface. Upon completion of the stress cracking test, results are often reported as failure time and percent of failure. ASTM 3350 classifies and codes ESCR of PE pipes and fittings at either 50% or 20% failure. Currently, code 4 represents the most resistance to slow crack growth, with a maximum failure probability of 20% at 600 h.

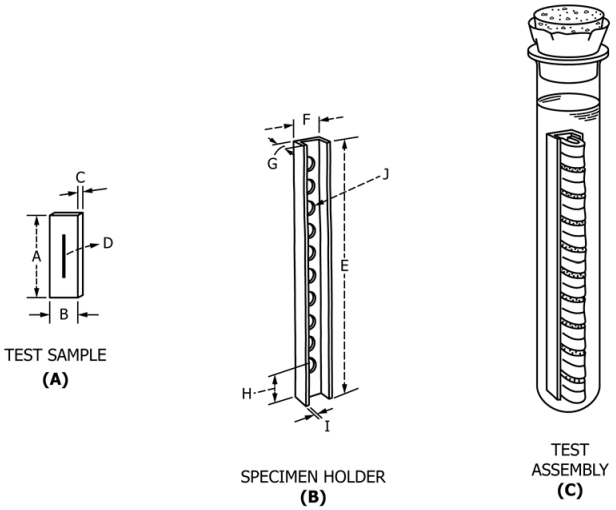


Figure 14. Schematic drawing shows the (A) razor blade notched sample, (B) sample holder, (C) multiple bent samples placed in specimen holder and inserted inside a glass tube filled with a thermally stable liquid for ESCR at 50°C or 100°C (Reprinted, with permission, from ASTM D F1693-21, Standard Test Method for Environmental Stress-Cracking of Ethylene Plastics).

*ASTM D2837-13: Standard Test Method for Obtaining Hydrostatic Design Basis for Thermoplastic Pipe Materials or Pressure Design Basis for Thermoplastic Pipe Products*

This method describes two equivalent procedures to obtain long-term hydrostatic strength (LTHS): the hydrostatic design basis (HDB) and the pressure design basis (PDB). The LTHS is determined by analyzing stress versus time-to-fail (rupture) data over a testing period up to 10,000 hours and extrapolating to 100,000 hrs (or even to 50 years (438,000 hours)) on a log-log basis. The method does include guidance on how to proceed with data that do not fall on a straight line. Similarly, the $LTHS_p$ is determined by analyzing pressure versus time data. ASTM D1598 describes the actual rupture test procedure, which is conducted under constant internal pressure and preferably at 40°C, 50°C, 60°C, 80°C, and 100°C, with a strong recommendation to include a test at 23°C for comparative purposes. The method precludes extrapolating values to temperatures beyond those tested or estimating performance in other similar materials.

The method requires a minimum of 18 failure stress/pressure-time data points for each environment (the minimum number of data points within each time frame in a factor of ten from 10 to 10,000 hours is listed in section 5.2.1, D2837). The purpose is to ensure the data points

are well distributed within the 10,000 hours range in the log-log scale to establish linearity. The data are analyzed by linear regression to yield a best-fit log-stress versus log time-to-fail straight-line equation. Using this equation, the material's mean strength at the 100,000 hours intercept is termed as LTHS or $LTHS_p$) and determined by linear extrapolation. The critical assumption of ASTM D2837 is that the experimental data will define a straight-line relationship according to the method's requirements, and this straight line can be extrapolated linearly beyond the experimental period, through at least 100,000 hours to determine $LTHS/LTHS_P$. The method also addresses data not meeting the straight-line assumption, such as high scatter or a "knee" (a downward shift from the initial set of straight-line data) where the $LTHS/LTHS_P$ would be underestimated or cannot be determined. Plastic Pipe Institute has analyzed over 3000 sets of data obtained with thermoplastic pipe and piping assemblies tested with water, natural gas, and compressed air. None of the current commercially offered compounds exhibited the "knee" non-linearity when tested at ambient conditions. However, some materials, when tested at higher temperatures, may show the "knee" before the minimum 10,000-hour requirement. In the case of PE piping materials, this test method includes a supplemental requirement for validating the linearity assumption. No such validation requirements are included for other materials where it is up to the user to determine, based on outside information, whether this method is satisfactory to extrapolate a material's $LTHS/LTHS_P$ for each specific combination of internal/external environments and temperature.

This test method is applicable to all known types of thermoplastic pipe materials and thermoplastic piping products. It is also applicable for any practical temperature and medium that yields stress-rupture data with an essentially straight-line relationship when plotting stress (or pressure) versus time of rupture on a log-log scale. In addition to the 100,000 hours related $LTHS/LTHS_p$, method D2837 also lists three procedures to further substantiate that the stress regression curve is linear to the 50 year (438,000 hours) intercept when it is desired to show that a PE material has additional ductile performance capacity (section 5.7 D2837).

*ASTM D1598-15a: Standard Test Method for Time-to-Failure of Plastic Pipe Under Constant Internal Pressure*

ASTM D1598 describes the actual test method determining the LTHS or $LTHS_p$ described in ASTM D2837 and hence HDB and PDB. Method D1598 covers the determination of the time-to-failure of both thermoplastic and reinforced thermosetting/resin pipes under constant internal pressure. This test method consists of exposing specimens of pipe to constant internal pressure in a controlled environment and temperature. Such a controlled environment may be accomplished by, but not limited to, immersing the specimens in controlled temperature water or air bath. Specimen pipe length between end closures shall be not less than five times the nominal outside diameter of the pipe, but in no case less than 12 inches. The 12-inch minimum specimen length requirement shall not apply to molded specimens. For larger sizes of pipe (>6 inches), the minimum length between end closures shall be not less than three times the nominal outside diameter but in no case less than 30 inches.

An end enclosure is attached to the pipe test specimen, and it is filled with fluid or air and conditioned at 23°C ± 2°C in a constant temperature environment before applying pressure and recording time to failure. Either free end closures or restrained end closures may be used, though D1598 acknowledges that the stress conditions are somewhat different for free-end versus restrained-end closures. For free-end closures, the caps are fastened to the specimen so that internal pressure produces longitudinal tensile stress in addition to hoop stress. The stresses of restrained-end closure specimens act in the hoop and radial directions only. Because of the difference in loading, the equivalent hoop stress in free-end closure specimens

of solid wall thermoplastic pipe is approximately 11% lower than in restrained-end closure specimens tested at the same pressure. Results are therefore suspect when pipe failure occurs within one diameter of end closure. A thorough examination must be conducted in that case to determine if failure is due to the end closure, and if so, the data must be discarded.

## 2.5 Analysis and Key Take-Aways on Design and Lifetime Assessment for Pipelines of Blended Hydrogen and Natural Gas

Having reviewed the state of existing natural gas pipelines, their materials of construction, how they are designed, how they fail, and how lifetimes are estimated, several aspects are apparent that are important relative to introducing hydrogen blends into the system.

Pipeline Materials:

Section 2.1 discussed the incumbent pipeline materials in detail. Pipe resin formulations have evolved over time, and their performance in hydrogen may vary significantly. The current pipeline network includes a wide variety of material vintages, along with a variety of service lifetimes. These variables introduce added complexity to evaluating the feasibility of blending hydrogen into the current pipeline network. To the best of our knowledge, relevant data in the technical literature are lacking. Investigation of how hydrogen effects may vary with different resin formulations, both vintage and modern, is warranted.

Pipeline Design:

While 49 CFR 192 includes transportation of “other” gases by pipeline, there are currently no federal regulations or safety codes and standards that relate to the specific challenges and material compatibility concerns regarding hydrogen gas transportation via polyethylene natural gas pipelines. New or modified standardized test methods may be needed. In particular, it may be prudent to verify the design pressure for pipes that will be distributing hydrogen blended gas by substantiating the HDB with the hydrogen-blended gas as the test medium. Revision to the standards governing this requirement and test method should be considered.

With joints being a major cause of failure, the effects of hydrogen on the joints are of particular interest, as described in Section 2.3.2. In addition, due to the difference in physical properties between hydrogen and natural gas, using current natural gas pipelines to transport hydrogen may or may not result in changes in the number of incidents or their severity compared to reported incidents. To assess this risk, further studies are needed on hydrogen leak rate through joints and mechanical testing of connected pipe sections; detection methods for joint defects and for leaks; and simulation approaches for hydrogen leaks and ignition.

Lifetime Assessment Methods:

Review of current lifetime assessment methods strongly suggests the continued use of ASTM test method D1598 to measure failure stress versus time to failure, and studies of the effects of hydrogen should include long-term tests of this type at the blend concentration anticipated. To mimic the actual condition of installed underground pipes, samples of restrained end-caps should be used. Results of these tests can be compared to published data on the performance of PE exposed to 100% natural gas to determine whether hydrogen shortens or extends pipeline life. These tests are lengthy (10,000 hours), so selecting the most appropriate PEs for the experiment is important.

Alternatively, test method F1473 with PENT specimens (an accelerated test at 80ºC and 2.4 MPa) could be used over a much shorter time frame (50 to 500 hours) to evaluate the effect of hydrogen on slow crack growth behavior, a process related to life assessment. A similar fast test for Slow Crack Growth Resistance (SCGR) has been published by international standard (ISO 18489) using cracked (notched) round bars under cyclic loading at 23ºC for molded PE or extruded PE pipes, especially for PE80 and PE100. Due to the large stress applied (10.5 to 13.5 MPa), the duration of this test is even shorter (less than 50 h). Unfortunately, neither of these two alternative methods can be used to estimate the LTHS at 100,000 hours or 50 years. However, these two methods do offer a reasonable means to evaluate hydrogen effects by comparing test results of specimens exposed to hydrogen with specimens not exposed to hydrogen.

In addition to direct strength measurement, international standard ISO-18488 is a new test that offers an indirect means to gain insight into the SCGR without long-term testing by using a strain hardening (SH) approach. Kramer and Brown reported SCG behavior in PE as a combination of yield stress and disentanglement of tie molecules in the craze zone where SCGR is directly related to the disentanglement[33, 34]. The method is even shorter in duration by using dumbbell specimens in tension at an elevated temperature of 80ºC. From the stress-strain curve, one can determine the strain hardening modulus using data of draw ratios between 8 and 12, where the modulus was proposed as a measure of resistance to fibril deformation related to tie molecules disentanglement. Dominguez, Carlos, et al. investigated the co-polymer effect on the SCG limit using a strain hardening test. They found very good agreement of SH modulus with PENT/FNCT (full notch creep test) data at low SCGR data but deviations at high SCGR when testing PE resins with either 1-butene or 1-hexene copolymer.[35] They attributed the difference to the location of short-chain branching in the two commercial resins made by different processes.

ISO-18488 is conducted at 80ºC, while ASTM D2837 for lifetime assessment is generally conducted at 23ºC for 10,000 hours or more. Like many physical properties of materials, one can conduct the (faster) strain hardening test at various temperatures and construct an Arrhenius plot of modulus versus 1/T to obtain an activation energy, assuming the mechanism is unchanged. In theory, the activation energy may be used to estimate the properties at different temperatures. Unfortunately, this approach to estimating lifetimes at lower temperatures by using data from accelerated tests at higher temperatures remains to be established.

# 3.0 Considerations of Hydrogen Use in Polyethylene Pipeline Distribution Systems

The literature relative to the effects of hydrogen/natural gas mixtures on PE is highly sparse. The permeation behavior of a 10% hydrogen/ 80% methane (resembles 90% methane-containing natural gas) blend was investigated on several commonly used PE pipeline materials in one study, [36] but effects of the gas blend on other PE properties has not been studied.

Review of the literature relative to pure hydrogen effects on PE reveals some data which we will now describe, highlighting the aspects that are relevant to pipeline design, failure modes, and lifetime. Data on hydrogen effects on mechanical, chemical, and physical properties is reviewed, followed by a discussion on hydrogen permeation and loss rates through the pipeline.

## 3.1 Mechanical Properties

### 3.1.1 Quasi-Static Tensile Behavior

#### 3.1.1.1 Elastic and Plastic Deformation Characteristics

Uniaxial tensile behavior is an important relevant performance metric, and investigations of the effects of hydrogen on PE commonly include uniaxial tensile testing. While data is limited, the effects of hydrogen pressure and concentration on the uniaxial tensile behavior of PE at room temperature and at elevated temperature conditions have been reported in recent years.[10, 11, 37, 38]

Alvine *et al.*[37] investigated the effect of high pressure hydrogen on the uniaxial tensile behavior of HDPE at room temperature by conducting *ex-situ* and *in-situ* tensile tests. *Ex-situ* experiments investigated the effect of rapid desorption of hydrogen from the saturated sample in ambient conditions. Tensile properties were observed to start to increase and recover to their original, unexposed values within 4 hours of removal from the hydrogen environment for thick samples (12.5 mm by 12.5 mm cross-section). This observation demonstrates the need to strongly consider hydrogen diffusion rate for *ex-situ* studies.[39] The *in-situ* investigation was carried out in the hydrogen pressure range from 28 to 35 MPa after 20 hours of soak time to saturate the sample. An 8% decrease in ultimate tensile strength was observed in 35 MPa hydrogen compared to specimens tested in air at ambient pressure. Furthermore, the study demonstrated a direct relationship between hydrogen pressure and tensile strength between 28 MPa and 35 MPa, with strength decreasing as hydrogen pressure increased. There was no observed influence on tensile modulus. The authors concluded that geometric swelling due to hydrogen absorption could not account for the observed decrease in strength; therefore, a plasticization effect or statistics may be responsible.

Menon *et al.*[40] investigated the *ex-situ* tensile properties of HPDE after exposure to 100 MPa hydrogen for sufficient time to saturate the polymer. The authors observed increases in tensile modulus, yield strength, and ultimate strength, which is in contrast to the *ex-situ* observations of Alvine *et al.* The differences in testing conditions between the two studies are as follows: (1) Menon *et al.* exposed HDPE to hydrogen at 100 MPa for 1 week, while Alvine *et al.* soaked at 28 MPa for 20 hours, which could result in different hydrogen concentrations for each study . The high pressure and long duration soak conditions of Menon *et al.*[40] could be sufficient to enable crystalline domain growth,[41] resulting in the observed increase in mechanical properties. (2) Menon *et al.* used relatively small cross-section samples that likely saturated rapidly at

ambient conditions. The brief *ex-situ* study of Alvine *et al.* using large 12.5 mm x 12.5 mm cross-section samples showed measurable change in mechanical properties within 4 hours after removal from high pressure conditions. It is likely that significantly shorter saturation and recovery times would be observed for the small samples of Menon et al. due to higher permeation rate compared to Alvine *et al.* for the rapidity of desorption relative to test durations. The rapidity of desorption relative to test durations could also explain the large scatter observed by Menon *et al.* in hydrogen charged samples. In contrast, the samples tested prior to exposure showed less scatter in the stress-strain curves and specifically measured properties (*i.e.* tensile modulus, yield strength, and ultimate strength).

Castagnet *et al.* conducted several *in situ* studies on low-pressure hydrogen effects (up to 10 MPa) on commercial PE (PE100) cut from sheet and pipe stock. These studies included tensile properties after short-term exposure (1 hr)[11] and long-term exposure (up to 1 yr)[10]. The authors concluded that no significant influence on mechanical properties was observed in any case, although some minor differences were noted. Tensile properties[11] were evaluated at 3 MPa and 10 MPa after soaking for 1 hr in hydrogen or nitrogen to saturate. There was no observable influence of hydrogen or nitrogen compared to tests conducted in air at ambient pressure. This may be due to insufficient saturation from a short exposure time at low pressure. Similar in-situ studies were conducted on PE after an initial exposure to 0.5 MPa or 2 MPa hydrogen for up to 13 months at temperatures up to 80°C[10]. The in-situ testing was then completed on the aged specimens at 3 MPa. A limited effect of exposure at higher temperature was observed and attributed to a slight increase in crystallinity, although the observed difference in mechanical properties was within the scatter of the data. There was no difference in mechanical results between PE exposed to 0.5 MPa and 2 MPa. The ultimate tensile strength of PE as a function of temperature when tested in-situ at a pressure of 3 MPa is shown below in Figure 15.

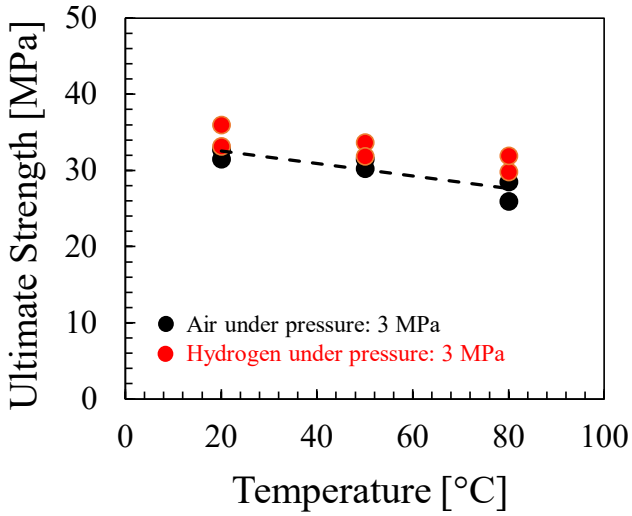


Figure 15. Effect of hydrogen (at 3 MPa pressure) on the uniaxial ultimate strength of HDPE at three temperatures. The ultimate strength reported corresponds to the first peak load; the entire load-displacement data was not provided in the paper.[10]

The combination of the *in-situ* experimental tensile data of Alvine *et al.* and Castagnet *et al.*[10, 11] shows that hydrogen pressure has some effect on HDPE, specifically a maximum reduction for both yield strength and the strain at the first peak load of about 15% at 35 MPa, as plotted in Figure 16. However, it also suggests that hydrogen pressure has a negligible effect on the uniaxial tensile behavior of HDPE at a service pressure below 3 MPa.[10, 11] Moreover, the minor reduction in the values in Figure 16 may be caused by the exposure to high pressure regardless

of the gases present (air, hydrogen, or nitrogen).[10, 11] The question of pressure effects specifically remains unclear and requires further investigation.

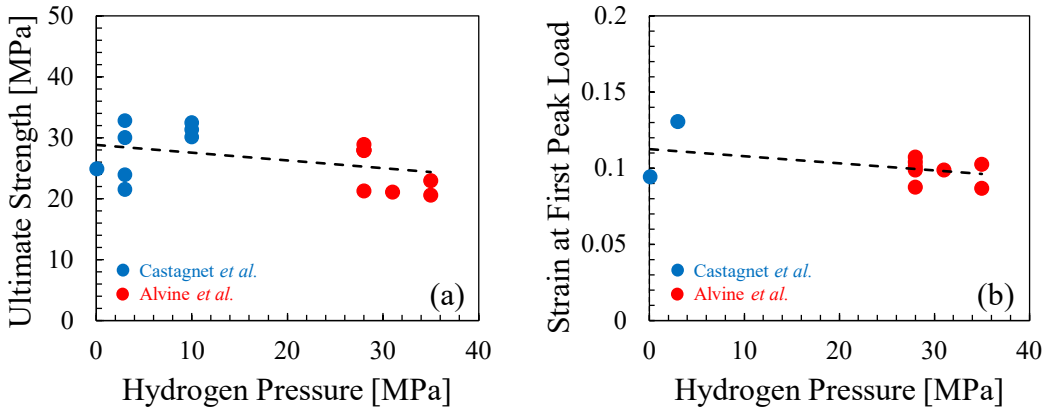


Figure 16. Effect of hydrogen pressure on the uniaxial tensile properties of HDPE at room temperature: (a) ultimate strength (b) strain at the first peak load.[11, 37]

#### 3.1.1.2 Effects of Defects

Defects (*e.g.*, blunt notch, sharp crack, etc.) play an important role in slow crack propagation, as discussed in Section 2.3.3. The effect of hydrogen on slow crack growth in the presence of defects is important but rarely studied in the literature. If hydrogen affects how the molecules disentangle, this would impact the slow crack growth and could be magnified in the presence of a large defect. Castagnet *et al.*[42] studied hydrogen effects on the fracture properties of HDPE through quasi-static tests on double end notch test specimens *in situ* at room temperature. Dissipated and released energies due to plastic deformation and damage were calculated by using the work-of-fracture method based on the entire evolution of load-displacement curves. Load-displacement curves were similar for HDPE as-received and exposed to 3 MPa hydrogen for most ligament widths; the largest deviation was observed in the widest ligament width (12 mm), for which hydrogen-exposed HDPE produced specific work of fracture around 270 kJ/m$^2$, whereas as-received HDPE was 220 kJ/m$^2$. However, considering all ligament widths tested, Castagnet *et al*. concluded that there was no noticeable effect of hydrogen on the dissipated and released energies as a function of the ligament area ahead of the crack tip during the fracturing process of the HDPE materials at room temperature. However, no data was found in the literature for the effect of hydrogen on other modes of fracture (*e.g.*, Mode II, mixed-mode, etc.), which involve different deformation processes that may be more sensitive to hydrogen effects.

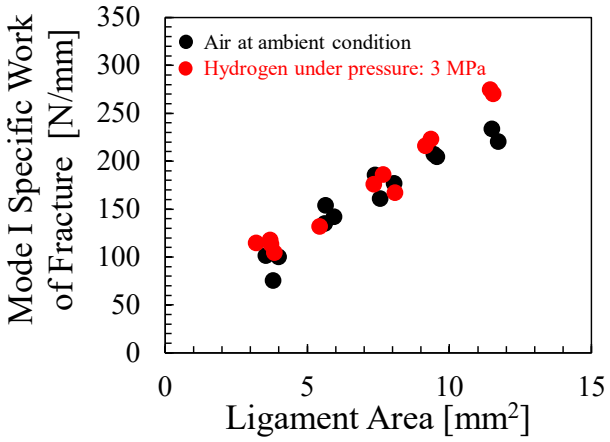


Figure 17. Effect of hydrogen (3MPa pressure) on the Mode I dissipated and released energies (*i.e.* specific work of fracture) as a function of ligament area at room temperature.[42]

.

### 3.1.1.3 Pipe Burst

While the foregoing studies focused the effect of hydrogen on specimens in a quasi-static loading condition, Simmons *et al.* [39] studied hydrogen effects directly on MDPE pipe subjected to burst testing at room temperature. In this study, ½ CTS pipe sections were exposed to pure hydrogen at 250 psi and room temperature for 72 hours. The pipes were removed from hydrogen exposure and hydrostatically burst. The time between removal from hydrogen and testing (interval time) was tracked to determine if the results would change as hydrogen diffused from the specimens. This data is shown in Figure 18. The interval time appears to have no significant effect on pipe burst pressure or maximum principal strain. All the investigated MDPE pipes after bursting showed similar fracture morphologies with ductile failure, as illustrated in Figure 18. The relationship between interval time and hydrogen concentration was confirmed with thermal desorption analysis. A specimen removed from hydrogen for 40 minutes would have approximately 40% of the hydrogen equilibrium concentration remaining in it.[39] These results indicate that hydrogen has a negligible effect on the failure behavior of the MDPE pipe.

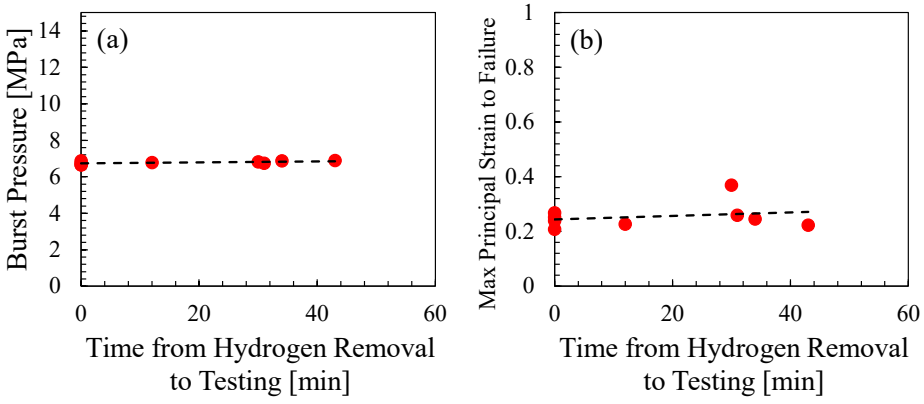


Figure 18. Effect of interval time on the following failure behaviors of the MDPE pipe: (left) burst pressure; (right) maximum principal strain at failure[43]. Note that the interval time means the time after taking the MDPE pipe with fully-soaked hydrogen from the hydrogen chamber.

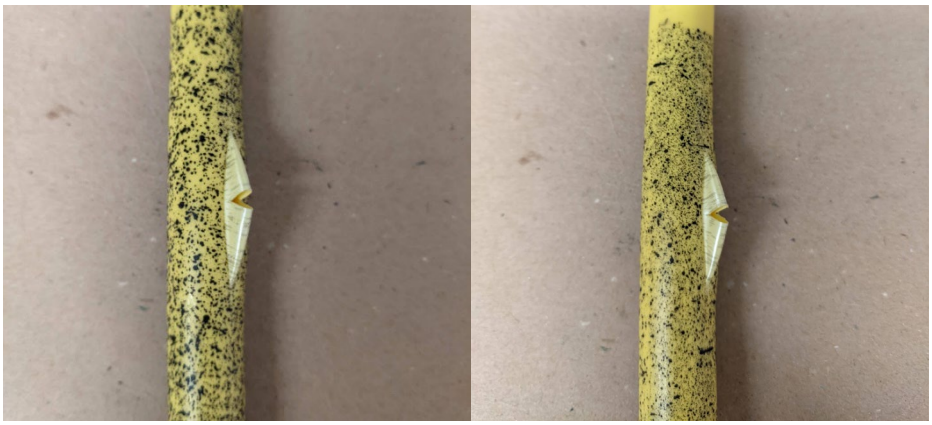

Figure 19. MDPE burst test specimens displaying ductile failure; (left) hydrogen exposed specimen; (right) control specimen not exposed to hydrogen[43]

#### 3.1.1.4 Hardness and Local Modulus of Pipe

Nanoindentation is a technique developed in the mid-1970s to measure the local mechanical properties of solid materials (*e.g.*, thin films, small volumes), including hardness, elastic modulus, viscoelastic properties/creep, fracture toughness, etc. Shaheer *et al.*[44] looked into the micro-mechanical properties across butt fusion welds of high-density polyethylene (HDPE) PE100 180 mm SDR11 pipes using the nanoindentation technique. They found that butt fusion welds exhibit a melt zone, where the material was melted during the welding operation, and a heat-affected zone, where the material was annealed, resulting in an increase in micro-mechanical properties. Chen *et al.*[45] employed nanoindentation to study the creep properties of the butt fusion-welded joint of HDPE pipes, often considered the weak point in a piping system. Their results suggested that creep failure usually occurs in welded joints in long-term service of HDPE pipes. Nanoindentation represents a means to probe how hydrogen exposure affects the local mechanical properties of piping materials, but it has not been applied frequently to date.

Simmons *et al.*[39] performed nanoindentation on MDPE pipe using a Nanovea M1 mechanical tester equipped with a standard nano-Berkovich tip. The MDPE specimens were exposed to 250 psi high purity hydrogen at room temperature for 72 hours, and nanoindentation was subsequently performed radially on the cross section of the pipe wall on specimens under three conditions: unexposed, immediately after pressure exposure, and 14 days after pressure exposure. Two important performance metrics were plotted as a function of the indentation location relative to the pipe wall outer/inner surfaces:

- hardness, which measures the resistance to localized plastic deformation induced by either mechanical indentation or abrasion. These types of localized plastic deformation are not uncommon during piping installation or repair;

- elastic modulus, which measures the resistance of a material to being deformed elastically (i.e., non-permanently) when a stress is applied to it.

The results shown in Figure 20 indicate that both hardness and elastic modulus drops after hydrogen exposure by 10-30%, but both metrics recovered to the pre-exposure levels 14 days after removal. The study also showed that high-pressure helium resulted in an increase in both modulus and hardness, in contrast to the decrease observed in hydrogen. Moreover, the

increase seemed to be relatively permanent, as no recovery was observed 14 days after the helium exposure.

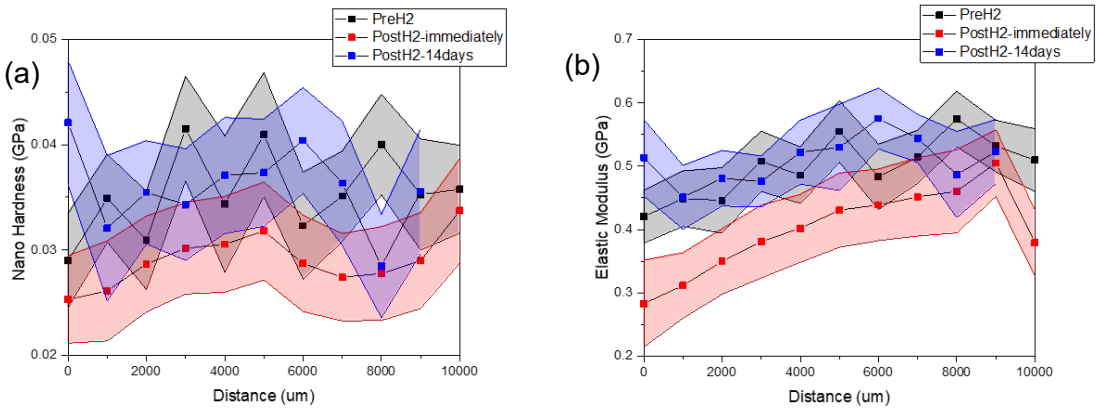


Figure 20. Hardness (a) and elastic modulus (b) profiles of a representative pipe specimen as a function of location through the thickness (inner wall edge = 0 μm while outer wall edge = 10,000 μm) before exposure to hydrogen (black), immediately after exposure to 250 psi hydrogen for 72 h (red), and 14 days after the exposure (blue)[43]

Further studies are needed to better understand this reversible change in hardness and modulus of MDPE pipes due to exposure to hydrogen, especially from a temporal perspective. Nanoindentation can be quite useful in studying local hydrogen effects on materials. Understanding the relationship between these property changes and the long-term performance of materials is of critical importance.

### 3.1.2 Fatigue Tensile Behavior

Fatigue response of a material is also an important aspect of mechanical behavior. Fatigue initiation, typically analyzed in the form of a stress-life (S-N) curve, of MDPE and HDPE materials at ambient conditions under different stress ratios and loading frequencies have been studied[46]. However, hydrogen effects on fatigue are relatively unexplored in the literature.

Experimental data for the effects of hydrogen pressure and concentration on fatigue initiation of notch-free PE materials was not found in the open literature. However, the effect of hydrogen on the fatigue initiation of the MDPE material in the presence of V-notches was investigated by Simmons et al.,[39] who conducted the fatigue tests on Circumferentially Notched Tensile (CNT) specimens at room temperature. The stress concentration factor at the V-notch tip was 5, the stress ratio was 0.1, and the loading frequency was 1 Hz. As illustrated in Figure 21, which shows maximum stress versus the number of cycles, the addition of hydrogen does not appear to significantly affect the fatigue lifetime at lower stress levels; the fatigue lifetime may be slightly affected at higher stress levels. However, it is still difficult to draw a solid conclusion about the effect of hydrogen on the fatigue behavior of PE materials due to (1) a lack of data for fatigue loading conditions with different stress ratios and loading frequencies; (2) a lack of data for fatigue (cyclic) crack propagation of material with a sharp crack, although there have been studies on the fatigue propagation of MDPE in air at different temperatures.[28]

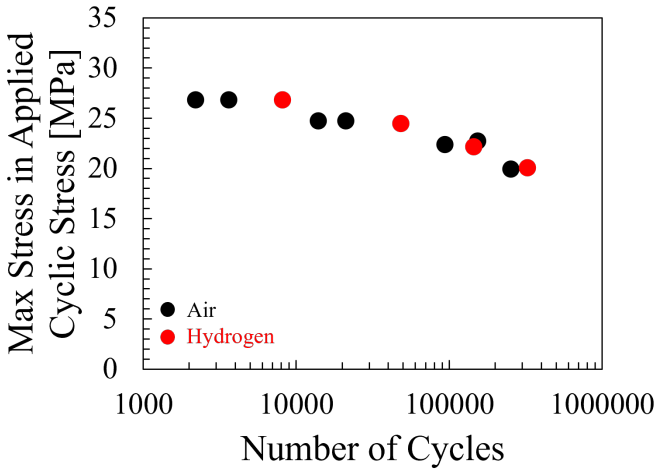


Figure 21. Effect of hydrogen on the stress-life curve (*i.e.*, maximum stress in applied cyclic stress vs. number of cycles) of MDPE obtained from Circumferentially Notched Tensile specimens[43]

### 3.1.3 Creep Tensile Behavior

Creep is another important long-term behavior of PE materials due to the long polymer chain structure. Understanding this mechanical behavior is essential for lifetime assessment of PE pipes, but hydrogen effects on creep are poorly reported in the literature. Castagnet *et al.* [42] investigated hydrogen effects on creep behavior of HDPE at room temperature. Due to the long duration of creep tests on dogbone specimens at room temperature at low constant stress levels (5MPa), the tests were conducted at different temperatures (20° to 60°C for 1 hour) to accelerate creep deformation. The creep master curve was constructed from the results following the time-temperature-superposition principle[47, 48] (TTS). Castagnet *et al*. found that HDPE exposed to hydrogen at 3 MPa exhibited slightly lower deformation compared to as-received material; however, the shift factor used to construct the master curve did not exhibit a noticeable difference between the specimens in ambient pressure air and those in 3 MPa hydrogen conditions. Hydrogen had only a minor effect on creep behavior, as plotted in Figure 22, showing similar evolutions of logarithmic strain for both air and hydrogen conditions.

The caveats on this conclusion are that the data was obtained from accelerated experiments at higher temperatures and at only one stress level. In addition, no experimental data for hydrogen effects on the creep behavior of specimens with pre-existing cracks or notches was found in the literature. Cracks and notches create regions with highly localized stress and can be important to how hydrogen affects the creep behavior of PE materials. More experiments on pre-notched or pre-cracked specimens exposed to hydrogen under different constant stress levels are recommended.

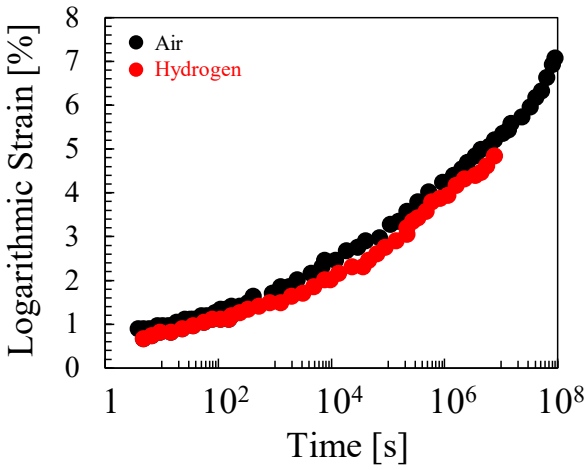


Figure 22. Effect of hydrogen on the evolution of logarithmic strain obtained from creep tests. Note that the results were constructed by using time-temperature-superposition principle[42, 47, 48](TTS).

## 3.2 Chemical and Physical Properties

Various characterization techniques have been used to understand the effects of hydrogen on PE pipeline materials. This section focuses on three aspects: degradation-induced pipe failure (Region III in Figure 6), physical properties of PE material exposed to hydrogen, and transport properties of hydrogen in PE pipe.

### 3.2.1 Degradation Induced Pipe Failure - Anti-Oxidant Depletion

#### 3.2.1.1 Oxidative Induction Time (OIT)

Polymers are formulated with antioxidants to increase their lifetime performance. Polyethylenes will auto oxidize over time. Antioxidants are used to mitigate the polymer damage. However, depletion of antioxidants is linked to the initiation of pipe failure, especially in the form of slow crack growth. The Oxidative Induction Time (OIT) is an indicator of an adequate antioxidant level remaining within a material. Dear and Mason[49] reported an asymmetric OIT profile through the wall thickness of a PE pipe used for chlorinated water transportation. OIT was lower at inner walls, where small axial cracks were observed. Further studies on the effect of chlorinated water on PE confirmed the decrease in OIT along with other forms of material degradation, such as a sudden decrease in ultimate elongation[50], formation of a porous layer observed under a microscope, decrease in average molecular weight, and increase in crystallinity[51].

The stress corrosion crack growth model developed by Choi et al.[52] based on crack layer theory suggests that crack growth rate and duration of stable crack growth correlate with OIT and are insensitive to further chemical degradation after depletion of antioxidants. Pinter and Lang [53] observed a slight decrease in creep crack growth at the beginning of the equilibrium crack growth stage with higher antioxidant concentrations[53], attributed to weaker microstructure with more additives.

In addition to strong oxidizers such as chlorinates, environmental conditions where the PE pipes are installed also affect the depletion rate of antioxidants, namely temperature[54], humidity[55],

exposure to leachate[56], soil acidity[57], solar radiation (especially ultraviolet light)[58, 59] and combined effects[60].

#### 3.2.1.2 Test Standards and OIT Results of Harvested PE Pipes

OIT is a relative measure of resistance to thermal-oxidative degradation for PE pipes. OIT is determined via differential scanning calorimetry (DSC) by measuring the time interval to the onset of exothermic oxidation at a specified temperature in an oxygen atmosphere. The test procedure is outlined in ASTM D3895 and ISO 11357-6. The isothermal temperature is chosen so that the OIT of differently degraded samples falls between minutes and a few hours. For PE resins, the isothermal temperature is typically 200 to 220°C. When choosing the optimal isothermal temperature, an oxidative induction temperature (OITP) test is performed on the same pipe section prior to the OIT test. OITP is determined during a heat ramp in an oxygen atmosphere. PE pipes must have an OITP above 220°C according to ASTM D3350.

The “onset of exothermic oxidation” is defined by two methods: tangent and offset. The tangent method is employed in most ASTM standards (D3895, D4565, E1858, D3350, D5885), where the oxidation onset is specified as the point of intersection (“t1” in Figure 23a) of the extrapolated heat flow baseline (“L1” in Figure 23a) and the tangent line at the inflection point of the exothermic peak (“L2” in Figure 23a). The offset method is introduced in ASTM D4565 and IEC 62582-4, both for polymeric insulations and jackets for electrical cables. According to the offset method, oxidation onset is obtained by shifting up the baseline (“L1” in Figure 23b) by a specified threshold (such as 0.05 W/g in Figure 23b) to intersect with the signal trace (“t2” in Figure 23b). For an autocatalytic oxidation reaction, the DSC peak associated with oxidation is detected as a major exothermic peak. The tangent method is preferred over the offset method according to ASTM D4565. In practice, the offset method is used when complex formulation and/or multi-step oxidative degradation is involved where the tangent method is not applicable.

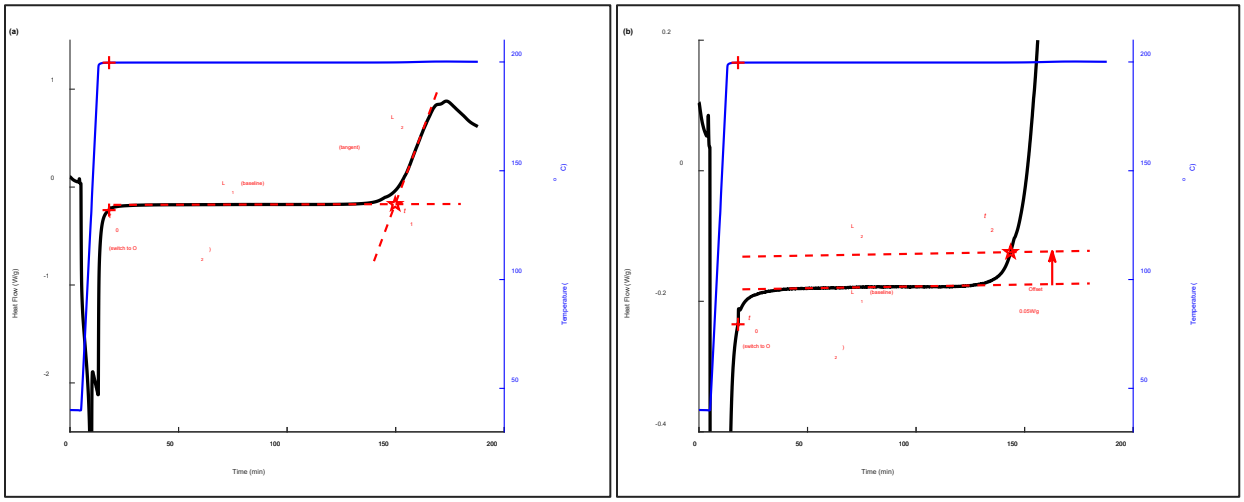


Figure 23. Oxidation onset is determined using (a) tangent method and (b) offset method.

Typical OIT values reported for harvested PE pipes installed in Australia and Algeria are plotted in Figure 24. OIT was obtained at the isothermal temperature of 210°C. EN1555-2 requires that PE pipes have an OIT at 210°C above 20 minutes. The weather conditions of the installation locations are listed in Table 4. Pipes from Algeria were from different regions in the country, but the specific location of each pipe was not reported[61]. Weather conditions in Algiers and Biskra listed in Table 4 are representative conditions for the north and south parts of Algeria[62].

In general, OIT decreases with service years. The decrease is faster in regions where the average summer temperature is higher. The PE80 pipe with an OIT of less than 10 minutes after nine years of service was used in the south of Algeria where the highest temperatures exceed 40°C[61].

Table 4. Average temperature and annual precipitation of the service locations of tested PE pipes.[62, 63]

| Location | Monthly Average Temperature (°C) | | Annual Average Temperature (°C) | | Annual Precipitation (mm) |
|---|---|---|---|---|---|
| | min | max | min | max | |
| Wodonga, Australia | 2.7 (Jul) | 31.1 (Jan) | 8.7 | 22.1 | 711.7 |
| Melbourne, Australia | 5.4 (Jul) | 26.6 (Feb) | 9.6 | 19.8 | 534.8 |
| Adelaide, Australia | 7.6 (Jul) | 29.5 (Feb) | 12.3 | 22.4 | 551 |
| Algiers, Algeria | 5 (Jan) | 33 (Aug) | 12 | 24.3 | 600 |
| Biskra, Algeria | 7 (Jan) | 41 (Jul) | 17 | 28.5 | 155 |

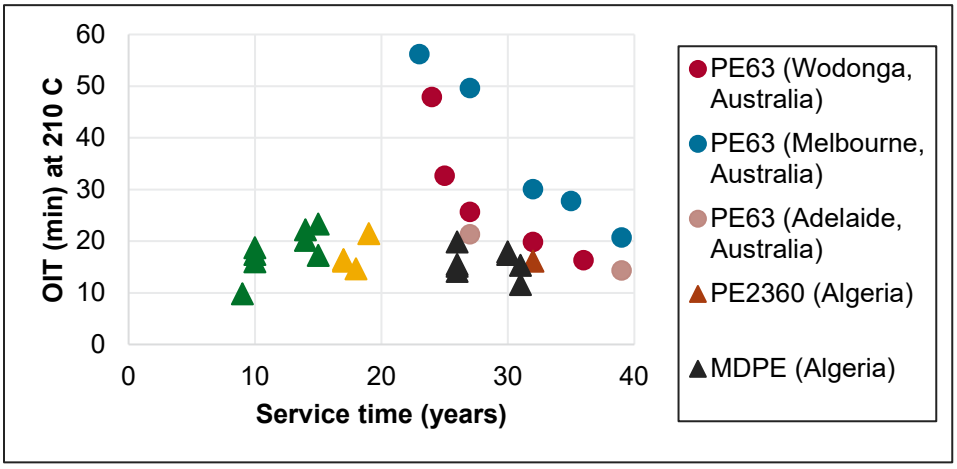


Figure 24. OIT at 210°C of harvested PE pipes used in Australia[62] and Algeria[62]

### 3.2.1.3 Prediction of Antioxidant Depletion Time

Depletion of antioxidants is the prelude to mechanical failure. A study on four grades of PE resins showed that mechanical properties decreased slowly (by less than 10%) when OIT was above 20 minutes and exhibited sharp decreases (tensile strength by 40%, Young's modulus by 30%, strain at break by 70%) when OIT approached zero.[64] Correlation between a catastrophic decrease in elongation at break and depletion of antioxidants was also reported for elastomeric polymers[65]. Silva et al.[63] also concluded that higher OIT PE implied better SCG resistance based on the Cyclic Pennsylvania Edge Notch Tensile (CPENT) test on harvested PE pipes from various locations. Due to variation in in-service conditions, the ranking of SCG resistance did not monotonically decrease with service life but correlated better with OIT. It was assumed

that the environmental factors that lowered the SCG resistance also accelerated the depletion of antioxidants, which rendered OIT an informative indicator for material failure.

#### 3.2.1.4 Antioxidant Depletion Kinetics

An overall first-order reaction kinetics[66] is predominately used for material lifetime prediction. Antioxidants functionalize as free radical scavengers. The elementary reaction between representative radical species $\mathrm{R}\cdot$ and the antioxidant $\mathrm{AH}$ is given in Equation (1).

$$\mathrm{R}\cdot + \mathrm{AH} \xrightarrow{k} \mathrm{RH} + \mathrm{A}\cdot \tag{3}$$

The reaction given in Equation (1) is assumed to be first-order, meaning the reaction rate is proportional to the concentration of reactants as given in Equation (2). The concentration of radical species $[\mathrm{R}\cdot]$ is a constant since it is abundant. The solution to Equation (2) is given in Equation (3), where $C_1$ and $K$ are constants. OIT is assumed to be proportional to the concentration of antioxidant $[\mathrm{AH}]$, which exponentially decays with aging time $t$.

$$-\frac{d[\mathrm{AH}]}{dt} = \mathrm{k}[\mathrm{R}\cdot][\mathrm{AH}] \propto [\mathrm{AH}], ([\mathrm{R}\cdot] \gg [\mathrm{AH}]) \tag{4}$$

$$\mathrm{OIT} \propto [\mathrm{AH}] = C_1 \exp(-Kt) \text{ where } K = \mathrm{k}[\mathrm{R}\cdot] \tag{5}$$

Service life is typically taken by extrapolating $\ln(\mathrm{OIT})$ vs. aging time $t$ plot to a threshold OIT, such as 0.5 min for PE[67], and finding the corresponding aging time $t$.

#### 3.2.1.5 Prediction from Accelerated Aging Conditions

Experimental estimation of the time to deplete antioxidants within a feasible timeframe of weeks or months requires accelerated aging at elevated temperatures and/or pressures. Arrhenius temperature dependency[68, 69] was assumed to model accelerated aging data. The Arrhenius model says the reaction rate constant (in this case, the apparent or overall rate constant $K$) depends upon temperature as in Equation (4), where $E_a$ is the activation energy, $R$ is the gas constant, and $T$ is the absolute temperature.

$$K = A_0 \exp(-E_a/RT) \tag{6}$$

Combining Equations (3) and (4), a straightforward method to calculate lifetime at a target temperature takes three steps: (i) calculating $K$ from the slope of a linear regression of $\ln(\mathrm{OIT})$ vs. $t$ curves at each test temperature, (ii) plotting $\ln K$ vs. $1/T$ and obtaining the new $K'$ at the target temperature $T'$ by linear regression, and (iii) plugging $K'$ back into Equation (3) and calculating the lifetime $t$ corresponding to the threshold OIT value. Alternatively, the time-temperature-superposition (TTS) method described in Section 5.3 can be applied to OIT isotherms. The TTS method is more widely used, especially when $\ln(\mathrm{OIT})$ vs. $t$ is not perfectly linear, i.e., the antioxidant depletion reaction is not strictly first order.

Elevated pressure can also accelerate degradation. Wang et al. introduced a pressure-dependent rate constant in the functional form of Equation (5):[70]

$$K = B \cdot \exp(-\frac{E_0}{RT} - \frac{\alpha P}{P_0 T} + \frac{\beta P}{P_0}) \tag{7}$$

where $B, \alpha, \beta$ = constants
$E_0$ = activation energy at reference pressure (1 atm)
$P_0$ = reference pressure (1 atm)
$K$ = overall reaction rate of antioxidant depletion

#### 3.2.1.6 Examination of Model Assumptions

Although the procedure described in this section has been widely used to predict polymer lifetime in oxidative degradation, deviations from this model behavior can arise from many aspects. Discussions regarding the validity of models are focused on three model assumptions: apparent/overall first-order kinetics, Arrhenius temperature dependence, and the OIT threshold value.

First, deviations from first-order can originate from many sources, including different types of antioxidants possessing different reaction order[71], loss of antioxidants through a physical process instead of chemical reaction[72], and zeroth-order depletion favored by basic autoxidation scheme[65, 68]. A more precise antioxidant depletion rate is given by Equation (6)[73], the solution of which is given in Figure 25.

$$r_{\mathrm{AH}} = -\frac{d[\mathrm{AH}]}{dt} = \frac{a[\mathrm{AH}]}{1 + b[\mathrm{AH}]} \tag{8}$$

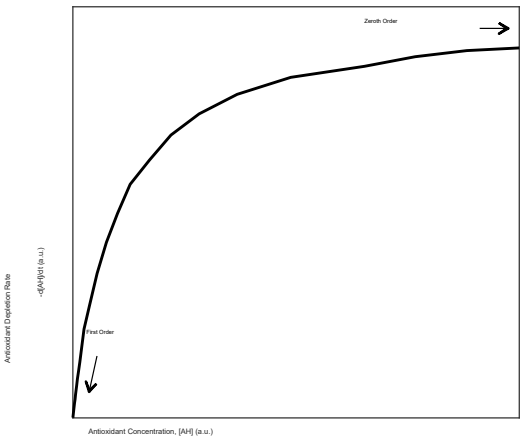


Figure 25. Rate of antioxidant depletion as a function of concentration based on Equation (5).

Nevertheless, experimentally measured antioxidant concentration is still best fit by a first-order decrease[65, 74, 75]. Justification for the apparent first-order antioxidant depletion is related to the low concentration of antioxidants[74], where the reaction is approximately first order, as shown in Figure 25. Loss of antioxidant by precipitation or volatilization, as measured by OIT profiling, also obeys first-order kinetics[76] and does not change the apparent reaction order.

The second assumption that reaction rate constant obeys an Arrhenius temperature dependence is also arguable. Two non-Arrhenius equations were proposed by Simon et al.[77], based on which the predicted service life was 1-2 orders of magnitude shorter than that by the Arrhenius equation. Even when the Arrhenius relationship is valid, the lifetime projected to the target temperature can still be inaccurate, as the activation energy $E_a$ could be different in different temperature ranges[78]. A practical way to examine if the same temperature dependence

is followed throughout the entire temperature range is by observing if isotherms can overlap while performing time-temperature superposition. If a lack of superposition is observed, it indicates a change in temperature dependence.

The third controversy is regarding the definition of an endpoint of a lifetime, whether in terms of a “critical antioxidant concentration”[79] (corresponding to a single-value OIT threshold) or a “critical oxidation level” (i.e., integral of oxidation products)[80]. The integral value is more directly derived from antioxidant depletion kinetics, while the OIT threshold is more convenient for pipe qualification.

#### 3.2.1.7 Effects of Hydrogen on Antioxidant Depletion Rate

This section describes three other effects on antioxidant depletion beyond the environmental stressors described in Section 3.2.1 related to transport of hydrogen and natural gas blends: (i) effect of hydrogen gas, (ii) effect of impurities such as oxygen, water vapor, $CO_2$, $H_2S$, and chloride gas, and (iii) effects induced by the heat fusion joining process.

Effect of hydrogen

Although it is well known that metal and metal alloys are prone to hydrogen damage[81], no such effect has been reported for PE pipelines degraded by pure hydrogen[36]. Hydrogen alone does not generate radicals that attack polymer chains[82]. Only one set of data was found pertaining to the effect of pure hydrogen. It was a four-year field test by Danish Gas Technology Center in Hørsholm, Denmark[12]. PE80 MDPE and PE100 HDPE natural gas pipes of different service histories were buried underground where the temperature was around 8°C. As shown in Figure 26, no decrease in OIT was found for pipes after four years of continuous exposure to pure hydrogen of 4 barg, even for the pipes with 20-year service history. In general, the PE100 pipes had higher OIT than the PE80 pipes investigated. This lack of degradation in the presence of pure hydrogen is positive relative to assuring the safety of pipeline transport of hydrogen/natural gas blends, but further tests on blends and at higher temperatures and humidities are needed.

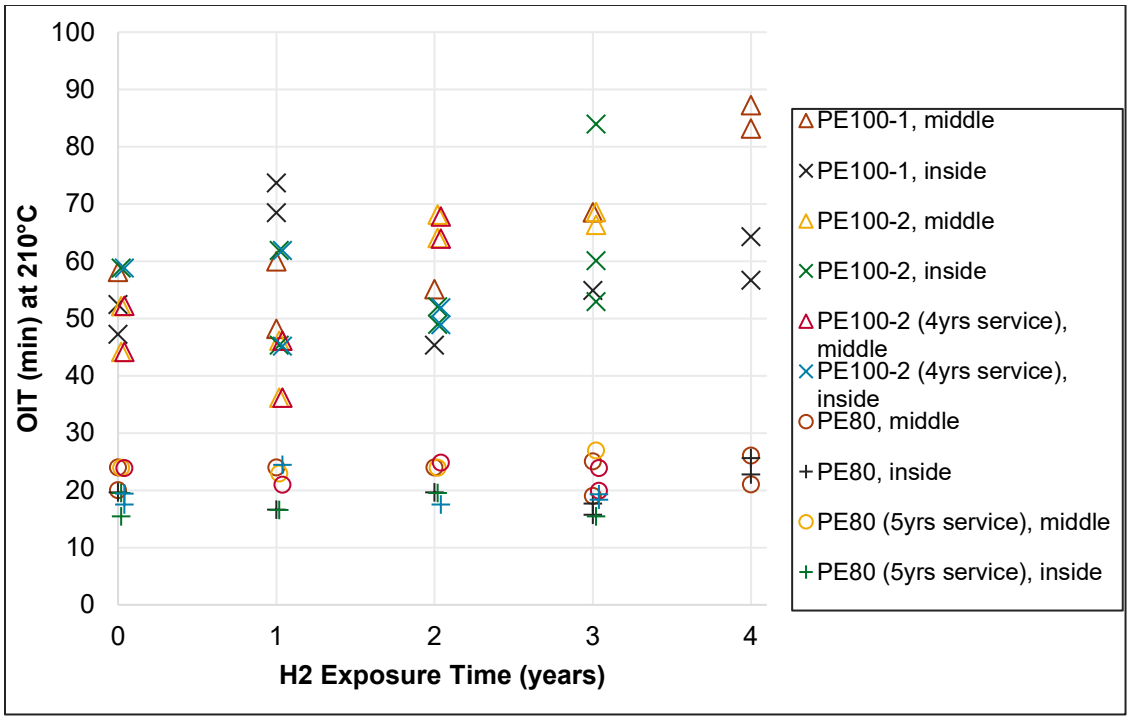


Figure 26. OIT of PE80 MDPE and PE100 HDPE pipes after four years of exposure to pure hydrogen at 4 barg and 8°C. X-axis locations are slightly shifted for discernability[12].

Effect of Impurities

Raw natural gas consists mainly of methane ($C_1$) and impurities, principally hydrocarbons ($C_2$ – $C_5$), water vapor, hydrogen sulfide ($H_2S$), carbon dioxide ($CO_2$), nitrogen, and helium. After gas processing, trace amounts of impurities are still present in pipeline gas, as given in Table 5. Whether the low-concentration contaminants will have catalytic effects on environmental degradation requires further study.

Table 5. Pipeline gas specifications[83]

| Characteristic | Specification |
|---|---|
| Water content | 4–7 lbm $H_2O$/MMscf of gas |
| Hydrogen sulfide content | 0.25–1.0 grain/100 scf |
| Gross heating value | 950–1200 Btu/scf |
| Hydrocarbon dewpoint | 14–40 °F at specified pressure |
| Mercaptans content | 0.25–1.0 grain/100 scf |
| Total sulfur content | 0.5–20 grain/100 scf |
| Carbon dioxide content | 2–4 mol% |
| Oxygen content | 0.01 mol% (max) |
| Nitrogen content | 4–5 mol% |
| Total inerts content ($N_2$ + $CO_2$) | 4–5 mol% |
| Sand, dust, gums, and free liquid | None |
| Typical delivery temperature | Ambient |
| Typical delivery pressure | 400–1200 psig |

It has been reported that OIT of MDPE pipes immersed in water decreased two to five times faster than those aged in air depending on the aging temperature from 40°C to 105°C[84], as a result of faster diffusion of antioxidants into surrounding hot water. In the case of gas pipelines, the theoretical assumption is that trace amounts of water provide little opportunity inside the pipes for this mechanism to occur.

The concentration of water or gaseous contaminants that leads to significant damage has not been well quantified, nor has their accumulated effects on antioxidant depletion over a timeframe of months to years.

Effect of Heat Fusion Joining

Heat fusion is standard practice for making joints with PE pipe and fittings in a field environment, as described in Section 2.2.2. It has been reported that fusion zones have higher crystallinity[85], lower orientation[85], lower Charpy impact energy[86], and lower ultimate elongation due to less plastic deformation[85-87]. The degree of reduction in mechanical properties depends on the grade of resin and the welding procedure[86]. Pipe and fitting faces to be joined are cleaned by wiping with solvents, heated to 260°C ± 6°C for several minutes, and held under pressure until sufficiently cooled. At such a high temperature, it is possible that antioxidants in the weld zone would be lost either through a chemical reaction and/or migration[76]. Whether this occurs needs further investigation via testing of OIT on PE resins at an isothermal temperature close to the actual welding temperature. Currently, OIT tests of PE are performed at 190-220°C, which is much lower than the welding temperature suggested in ASTM F2620 (260°C). In addition to testing the average OIT, the profile of OIT near the joint is also informative to reveal the depth of the affected zone. In a study by Haroon[76] of two PE pipes, the OIT of an ELTEX pipe was lower in the surface and bore regions than the middle portion, while the OIT of the other pipe made of RIGIDEX resin was homogeneous across its thickness, as shown in Table 6. The OIT of ELTEX and RIGIDEX resins are given in Table 7. The type of resin may have different resistance to loss of antioxidants during heating.

Measurement of OIT profiles in a variety of resin systems are needed. OIT profiling data would be useful for estimating the risk of potential depletion of antioxidants in fusion zones that will cause loss of mechanical properties, embrittlement, or cracking.

Table 6. OIT profile of weld zone of PE pipes[76]

| Sample | Location | OIT (min) at 200°C |
|---|---|---|
| ELTEX Tub 124 180mm OD | Surface | 26 ± 22.9 |
| | Mid | 116 ± 8.6 |
| | Bore | 39 ± 3.9 |
| RIGIDEX 002-50 180mm OD | Surface | 77 ± 14.6 |
| | Mid | 77 ± 12.2 |

| | | |
|---|---|---|
| | Bore | 72 ± 8.1 |

Table 7. OIT of PE resins[76]

| Resin | Sample Color | OIT (min) at 200°C |
|---|---|---|
| ELTEX | Blue | 177 ± 4.2 |
| | Black | 70 ± 3.2 |
| | Orange | 218 ± 2.3 |
| RIGIDEX | Blue | 89 ± 2.7 |
| | Black | 57 ± 3.4 |
| | Yellow | 81 ± 1.8 |

In summary, OIT is an informative measure of antioxidant depletion that is correlated with the service life of pipes. However, there is limited data directly pertaining to the effects of pure hydrogen or blended hydrogen with the impurities in natural gas on the antioxidant depletion rate of PE pipelines. Further investigation on OIT and OIT profiles is needed, especially on pipes subjected to hydrogen exposure, field service, and heat fusion joining.

### 3.2.2 Physical Properties

#### 3.2.2.1 Crystallinity and Density

Degree of crystallinity (DOC) is an important intrinsic property of polymers, and even slight changes can impact mechanical performance and service life. DOC can be reliably obtained from wide-angle X-ray diffraction (WAXD) methods and differential scanning calorimetry (DSC). In the case of WAXD, DOC is a ratio of the areas of the crystalline peaks to the sum of the areas of the crystalline peaks and the broad, amorphous peak. In the case of DSC, DOC is obtained from the ratio of the melting enthalpy obtained from the experiment to the theoretical heat of fusion of 100% crystalline polyethylene.[88-90]

The importance of crystallinity of PE pipes as a useful parameter in determining remaining useful life was highlighted by Frank and co-workers.[91] Similarly, studies pertinent to pressurized hydrogen (0 to 13,000 psi) exposure to various PE materials (including pipes) were performed by Fujiwara and co-workers[41, 92], and Menon and co-workers[40] (see Section 6.2.4.3 for the effect of crystallinity on permeation and solubility). The degree of crystallinity[41, 93, 94] as a function of hydrogen pressure for various PE materials is summarized in Figure 27a. In summary, all the materials studied demonstrated a 3 to 5% increase in crystallinity after exposure to high-pressure hydrogen (13,000 psi). Fujiwara and co-workers also reported that decompression to atmospheric pressure restores the original crystallinity and verified that the high-pressure hydrogen exposure effect on the crystallinity of PE was similar to that of hydrostatic pressure. On the contrary, Simmons and co-workers[39] reported a 2% decrease in crystallinity after low-pressure hydrogen exposure (0 – 250 psi) for MDPE pipe materials (see Figure 27b).[39, 43]

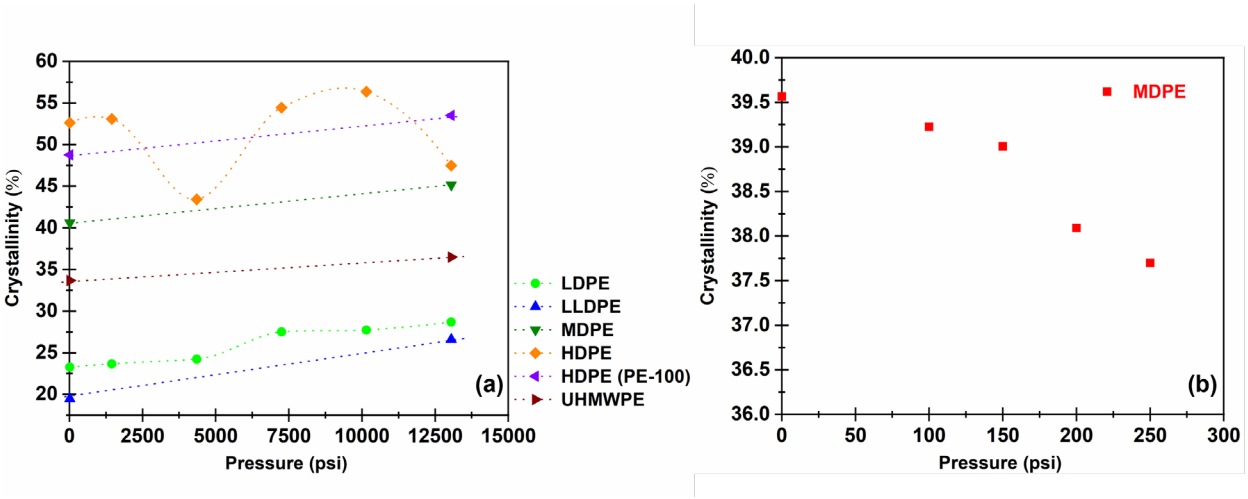


Figure 27 (a)Degree of crystallinity as a function of hydrogen pressure for various PE types[41, 92, 94] and (b) MDPE pipe material[39]

Overlaying density alongside crystallinity is helpful in understanding the available free volume in the amorphous phase in semicrystalline polymers[95, 96]. The importance of free volume and its effect on diffusivity and permeation of hydrogen in PE is highlighted in section 6.2.4.3. Experimentally, density is usually estimated by using Archimedes principle[97], and the densities[41, 92, 94, 97] as a function of high-pressure hydrogen (up to 13,000 psi) exposure are summarized in Figure 28a. The densities of all the PE types tested resulted in a 3 to 5% increase in density at the highest hydrogen pressure (13,000 psi). Fujiwara and co-workers[41, 92, 94] also reported that the increased densities reverted back to their baseline values after depressurization, which indicates that no permanent change in density was observed. On the contrary, Simmons and co-workers reported a 3.5% decrease in density for MDPE exposed to low-pressure hydrogen (0 to 500 psi).

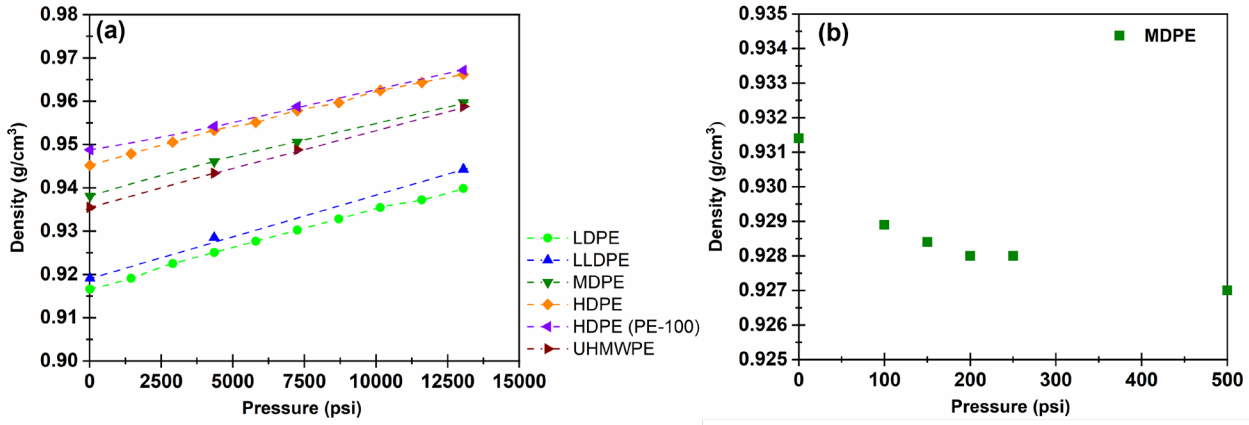


Figure 28 (a)Density as a function of hydrogen pressure for various PE types[41, 93, 94] and (b) MDPE material[39]

In summary, although comprehensive studies have been performed to evaluate crystallinity, morphological understanding of changes in crystallites caused by hydrogen exposure is lacking.

In addition, comparative studies with in-service pipe samples and with both unimodal and bimodal resins to understand their behavior under hydrogen exposure are also warranted.

#### 3.2.2.2 Damage

Imaging is frequently used to detect and assess damage in polymeric materials. To assess damage in PE materials due to hydrogen exposure, Fujiwara and co-workers [98] used light transmission methods and X-ray computed tomography (X-ray CT). In the light transmission method, a microscope with a charge-coupled device camera and an LED light source was used. The transmitted light after passing through the specimen with or without damage was recorded. Specifically, the extent of destruction $\xi$ was quantified by using the mean of the brightness (BR) values of red, green and blue (RGB) before and after hydrogen exposure:

$$\xi = 1 - \frac{BR_{before\ exposure}}{BR_{after\ exposure}} \tag{9}$$

where $\xi$ is the extent of destruction, $BR_{before\ exposure}$ is the the brightness value before exposure and $BR_{after\ exposure}$ is the brightness value after exposure.

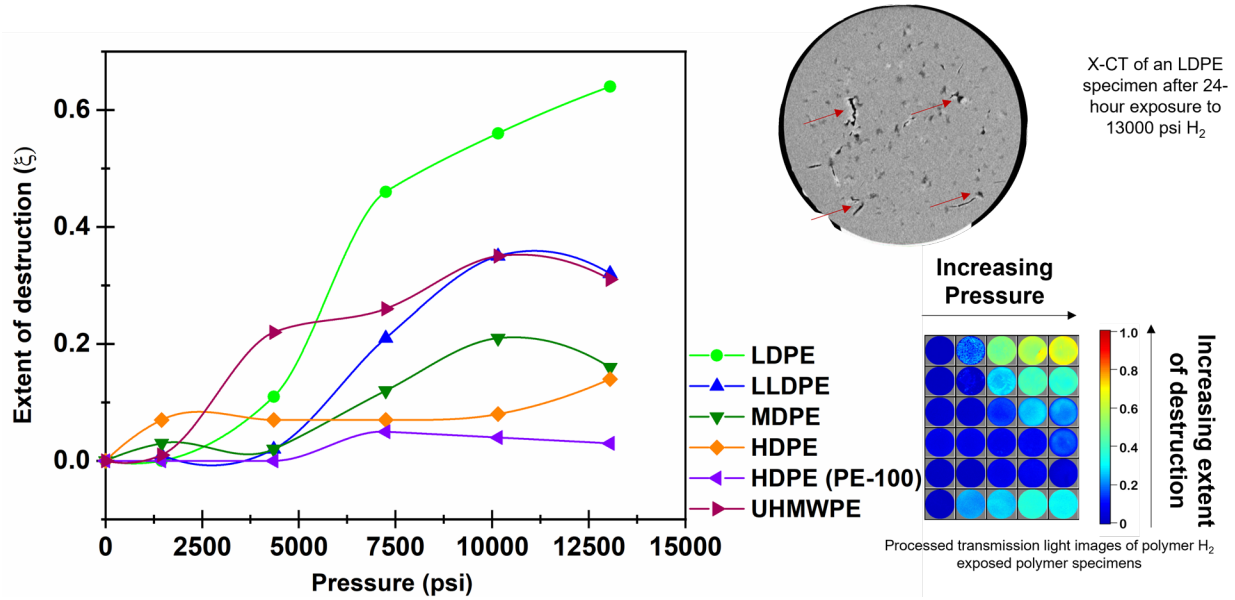


Figure 29 Extent of destruction as a function of high-pressure hydrogen (left). Processed transmission light detection images (shown as a matrix) for PE disk specimens (right). X-ray CT image showing voids and damage on an LDPE disk specimen after 24-hour exposure to 13000 psi hydrogen (top right)[93, 94]. Images are modified and re-used with permission from Elsevier

The extent of destruction as a function of pressure is summarized in Figure 29. In addition, processed images of various PE disks are also shown. LDPE was reported to have the highest

extent of damage (also confirmed by the X-ray CT scan shown in Figure 29), with the extent of destruction being significant in the center of the sample. HDPE (PE-100 pipe material) was reported to have demonstrated the least damage. The extent of damage was also reported to be dependent on the degree of crystallinity of the material; the material with the lowest crystallinity demonstrated the most damage, and the material with the highest crystallinity demonstrated the least damage. This is mostly because within the crystalline phase in a polymer the chains are packed in a much higher order than the amorphous, which inherently limits the dissolution of hydrogen by limiting the free volume.

In summary, non-destructive techniques like light transmission and X-ray CT are useful in assessing microscopic level damage to the exposed specimens. Future studies should focus on utilizing the aforementioned imaging techniques in conjunction with mechanical testing; such data is valuable in creating a diagnostic tool for studying PE pipe materials for internal wall damage and crack initiation tip geometries.

## 3.3 Hydrogen Losses Through Pipeline Permeation

Hydrogen is a small molecule that has relatively high mobility in solids. As such, permeation rates from pipelines during normal operation (that is, in the absence of major physical defects or leak pathways) will be inherently higher than natural gas and may occur through different mechanisms. The potential for significant losses of hydrogen from the natural gas distribution system should be considered as part of the overall evaluation of this option. This section reviews the literature for what is known about hydrogen permeability in pipelines as well as its impacts from an environmental and economic perspective.

Hydrogen is a “greenhouse gas”, and the global warming impacts of leakage from a future hydrogen-based energy system are being considered.[99] The magnitude of these impacts depends, of course, on the total amount of leakage in current hydrogen infrastructure and systems. While some researchers have assumed a 10% hydrogen leakage rate[99], there is very limited data available in the literature, and there are few tools to accurately measure hydrogen leakage *in situ*. Tromp et al. [100] pointed out that estimates of hydrogen leakage rates of 10% to 20% are based on early analysis of early-generation, small-scale hydrogen delivery systems and are not consistent with other studies that have measured and projected rates of less than 1% to 2% and up to 10% only in extreme cases.

What losses due to permeation through the body of a PE pipeline are credible, that is, without consideration of joints, valves, etc.? In a preliminary study, we analyzed the permeation rates of both pure hydrogen and pure methane in three common piping materials: MDPE, HDPE, and PA11. We applied Darcy’s law[101] and assumed an Arrhenius temperature dependence of gas permeability. Permeation rates for both hydrogen and natural gas for these three materials are estimated and summarized in Table 8.

Table 8. Estimated hydrogen and methane permeation rates in HDPE, MDPE, and PA11[102] [103]

| | Permeation rate of hydrogen gas [mol $H_2$/ (m·s·MPa)] | Permeation rate of methane gas [mol $H_2$/ (m·s·MPa)] |
|---|---|---|
| HDPE | $9.2\times10^{-10}$ | $3.2\times10^{-10}$ |
| MDPE | $3.1\times10^{-9}$ | $1.4\times10^{-9}$ |
| PA11 | $4.7\times10^{-10}$ | $2.6\times10^{-11}$ |

Total US natural gas consumption in 2020 was $30.47\times10^{12}$ mol[104]. We assumed that the gas pipes are IPS6, DR11 (the outside diameter is 168.3 mm and the wall thickness is 15.29 mm) with a total cumulative length of $2.4\times10^{6}$ km. The resulting volume of hydrogen gas loss per year at various temperature and pressure conditions are shown in Fig. 30. The service pipeline temperature ranges from 240 K to 327 K [105] Hydrogen loss rates vary exponentially with temperature and linearly with pressure. Under the most severe service temperature of 320 K and pressure of 10 bar, the hydrogen volume loss rate in MDPE, HDPE, and PA11 are 0.066, 0.019, and 0.011 [%/year]. Again, this is simply for permeation through the body of the pipe and excludes other sources of leakage, such as valves, mechanical connectors or the permeation of welded joints.

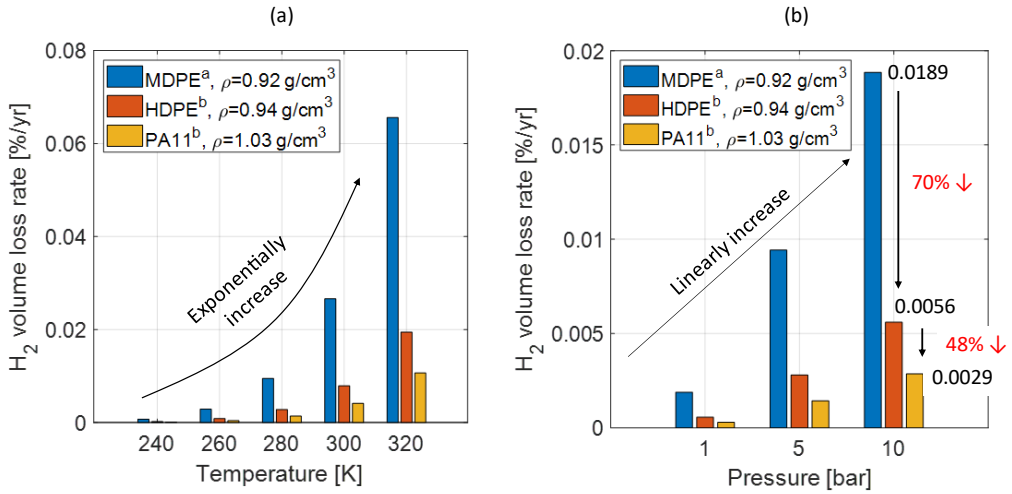


Figure 30. Hydrogen gas volume loss rate per year. (a) the temperature effect at 10 bar. (b) the pressure effect at 293 K[106]

### 3.3.1 Mechanisms of Gas Permeation

~~as~~ permeation is a complex physicochemical process of sorption, diffusion, and desorption of gas molecules. The permeation of gases is usually described in terms of a “solution-diffusion” mechanism, which is the key process that determines the permeation properties. The gas transport process can be divided into five successive steps (Figure 31):[107]

1. The gas passes the limit layer of gas from the high-pressure side by diffusion.

2. The gas is absorbed by the polymer through chemical affinity or solubility.

3. The gas diffuses through the polymer.

4. The gas is desorbed on the low-pressure side.

5. The gas passes through the limit layer on the low-pressure side by diffusion.

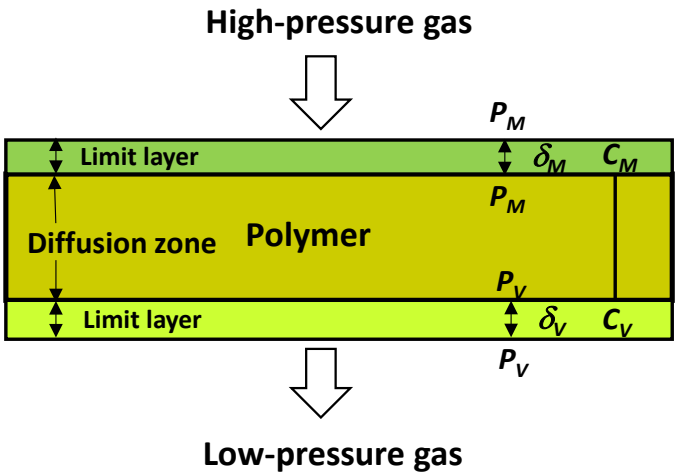


Figure 31. The diffusion mechanism of gas in the polymer, modified with permission from ref[107]

Step 1 and step 5 are generally rapid and can be neglected from an analysis of kinetics, leaving the transport process governed by absorption, dissolution, diffusion, and desorption. Dissolution is strongly dependent on the solubility *S,* which in turn depends on the interaction between the gas penetrant and the polymer and on gas pressure. Diffusion depends on the mobility of the gas penetrant in the polymer, expressed by the diffusion coefficient, *D*. The gas permeability coefficient *P* is expressed as $P = D \times S$ and reflects both of those processes.

#### 3.3.1.1 Permeability

Gas permeability was initially defined by Barrer *et al*. using a differential pressure method[108]. Gas permeability measurement using the method has been standardized in ASTM 1434 and ISO 7229 for oxygen, nitrogen, carbon dioxide, air, and helium. This method uses a high-pressure cell and a low-pressure cell separated by a polymer membrane. The amount of gas permeated per unit time is measured until the penetrated gas reaches a steady state, and the flux aper permeation area considering test temperature and the test pressure is expressed as a gas permeability coefficient, *P*. After normalized by polymer thickness (*d*), *P* is expressed by the following equation.

$$P = \frac{273.15 \times V \times d}{A \times Dp \times Tx\ 0.0227} \quad (10)$$

Where *d* is the thickness of the membrane (m), *V* is the amount of hydrogen permeating through the membrane per unit time at the steady-state ($cm^3$/sec), *A* is the permeation area ($m^2$), $\Delta p$ is the pressure difference between the two sides of the membrane (Pa), and *T* is the temperature (K).

#### 3.3.1.2 Diffusivity

A simple method to concurrently estimate *D* when *P* is determined using the method described above is based on the delay between the start of the test and when hydrogen begins to appear in the low-pressure cell. Specifically, the so-called delay time $\theta$ is determined by plotting concentration vs. time in the low-pressure cell and extrapolating the linear portion of the

concentration curve (i.e., during steady-state diffusion) to the x-axis. The x-intercept yields $\theta$ that can in turn be used to estimate *D* as:

$$D = \frac{d^2}{6q} \tag{11}$$

There are two other non-equilibrium methods: thermal desorption analysis gas chromatography (TDA-GC) and a volumetric collection (VC) method using a graduated cylinder upside down.[109] Calculation of the absolute mass of hydrogen charged in a sample from a GC measurement requires GC sampling volume (column volume) *V*, the flow rate of the carrier gas in the GC system, the temperature, and the pressure of the sample in the sample loop. The number of moles of hydrogen in the mixed gas (with carrier gas) should be calculated from the GC-measured concentration using the ideal gas law, *PV* = *nRT*. [110]

The TDA method treats the system as non-equilibrium diffusion from a sample of uniform initial concentration that follows Fick's second law, i.e.

$$\frac{\partial C}{\partial t} = D\Delta C \tag{12}$$

A sample with (assumed) uniform initial hydrogen concentration is placed in a chamber with a gas flowing through it. The outlet gas is sampled periodically and measured by GC. The concentration of the outlet gas will decay at a rate related to the solution to equation 11 for the sample geometry (e.g., a Bessel function solution for a sample with cylindrical geometry), which will include the diffusion constant *D* and the (known) sample dimensions. The concentration vs. time curve can then be fit to estimate *D*.

The whole procedure is as follows: hydrogen dissolved in plastics under high pressure is released into the air due to the pressure difference when the pressure vessel is decompressed. Assuming that the hydrogen is initially distributed uniformly in a cylindrical type sample and diffuses into the air, the change in the hydrogen gas residue $C_t$ in the samples is a function of time *t* and expressed as follows,

$$C_t = \frac{32}{\pi^2} C_0 \left[\sum_{n=0}^{\infty} \frac{exp^{(-(2n+1)^2\pi^2 Dt/z^2)}}{(2n+1)^2}\right]\left[\sum_{n=1}^{\infty} \frac{exp^{(-D\beta_n^2 t/r^2)}}{\beta_n^2}\right] \tag{13}$$

where $C_t$ is the remaining hydrogen content (ppm), $C_0$ is the total charged amount of hydrogen into rubber in the unit [wt·ppm], *n* the number of the terms, *D* is diffusion coefficient ($m^2$/sec), *z* is the thickness of the sample, and *r* is the radius of sample. $\beta_n$ is the root of the zero-order Bessel function: with the first six roots of $\beta_1$ = 2.405; $\beta_2$ = 5.524; $\beta_3$ = 8.654; $\beta_4$ = 11.792; $\beta_5$ = 14.931; $\beta_6$ = 18.071) sufficiently accurate values can be computed readily for most values. Equation (9) is the solution of Fick's second law of diffusion for a cylindrical sample. The *D* and $C_0$ are obtained by Eq. (9) from the experimental CR(t) data.

In the VC method, the hydrogen released from samples is collected in a submerged, inverted graduated cylinder, and gas volume is recorded as a function of elapsed time. The volume of hydrogen, $v_H$ ($cm^3$), is converted into mass concentration of hydrogen, C (wt ppm) at 1 atm and 295K using the ideal gas equation.

$$C\ (wt\ ppm) = V_{H\ (cm^3)}\ x\ 4.131\ x\ 10^{-5} mol\ x\ \frac{2.018\ g/mol}{m_{sample}\ (g)} \quad (14)$$

#### 3.3.1.3 Solubility

At moderate pressures (1 to 10 MPa), hydrogen solubility generally follows Henry's Law, i.e.

$$S = k(T) \times P \quad (15)$$

The solubility (the equilibrium concentration) *S* is directly proportional to the partial pressure of the hydrogen P, and the proportionality coefficient *k* is a temperature-dependent constant[111, 112]. However, there can be a severe deviation from this ideal, linear behavior at higher pressures, particularly if hydrogen begins to affect polymer morphology.

The solubility coefficient, S, can be simply determined using the relationship among the three coefficients measured using the permeation test above, as shown in the following equation.

$$S = \frac{P}{D} \quad (16)$$

Another method is to use a total amount of hydrogen in the pressure range of 2 to 11 MPa. In this range of pressure, the total amount of released hydrogen data approximately follows Henry's Law, and the hydrogen solubility (*S*) of each sample is then obtained from the slope of the linear curves of $C_0$ (wt ppm) vs. pressure (MPa).[109, 110]

$$S\left[\frac{mol}{m^3 MPa}\right] = \frac{slope\ \left[\frac{wt\ ppm}{MPa}\right] 10^{-6}\ x\ d\left[\frac{g}{m^3}\right]}{m_{H_2}\left[\frac{g}{mol}\right]} \quad (17)$$

where $m_{H2}$ is the molar mass of hydrogen (2.018 g/mol) and d is the density of the sample.

In the work done by Yamabe and Nishimura, solubility results obtained from both the TDA and VC methods were consistent with each other within experimental uncertainty. Hydrogen solubility of several different polymer materials obtained from different reports were comparable to one another.[113]

#### 3.3.1.4 Factors Affecting Hydrogen Permeability, Diffusion, and Solubility

The permeability, diffusivity, and solubility of gases in PE polymers are primarily affected by pressure, temperature, and material morphology and composition (crystallinity and fillers). This section briefly reviews what is known about those effects.

Pressure

At low pressures, pressure does not significantly affect gas permeability. For example, Naito et al. found that the hydrogen permeability of LDPE in the range from 2 to 8 MPa[114] showed no apparent pressure dependence. However, there is increasing interest in operating hydrogen gas refueling systems at pressures up to 90 MPa, where behavior may become non-linear.[115, 116] Fujiwara et al. developed a steady-state high-pressure hydrogen gas permeation test (HPHP) to measure hydrogen permeability of high density of polyethylene (HDPE) in a high-pressure environment at 30 °C.[92] Experimental results indicate that hydrogen permeation rate increases with increasing pressure, but at higher pressures the apparent permeability gradually decreases (Figure 32a). This deviation from Henry's law at high pressure suggests a decrease of free volume by polymer chain segments, which inhibits the process of diffusion and reduces the apparent permeability coefficient.[82, 117] The crystalline region of PE also inhibits the diffusion of hydrogen in a high-pressure hydrogen environment.[118] Interestingly, the permeability coefficient, diffusion coefficient, and solubility coefficient all decrease when hydrogen pressure increases. The hydrogen permeation rate (at constant temperature) more strongly affected by the diffusion rate than solubility (Figure 32c and 2d).

Thermal desorption analysis of hydrogen on medium density polyethylene (MDPE) after exposure to low hydrogen pressures (100 - 500 psi) showed a gradual increase of equilibrium hydrogen content ($C_0$) and a decrease in diffusion coefficient ($D$) with increasing hydrogen pressure, in good agreement with the literature as shown Figure 33.[41] Crystallinity and density measured immediately after decompression decreased with increasing hydrogen pressure.[39] The crystallinity and density of exposed MDPEs slowly recovered with time.

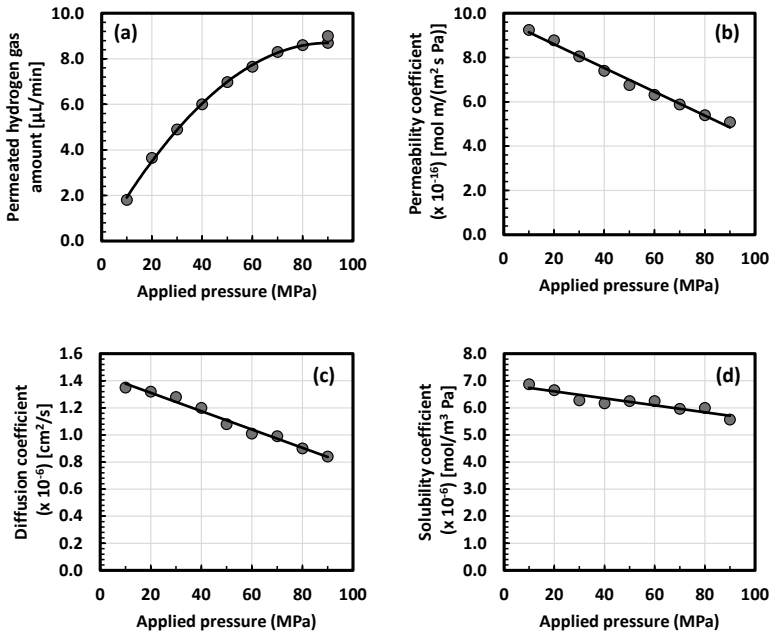


Figure 32. Effect of applied pressure on permeation testing at 30°C: (a) hydrogen permeation rate, (b) apparent permeability, (c) diffusivity, (d) solubility. Modified with permission from ref.[92]

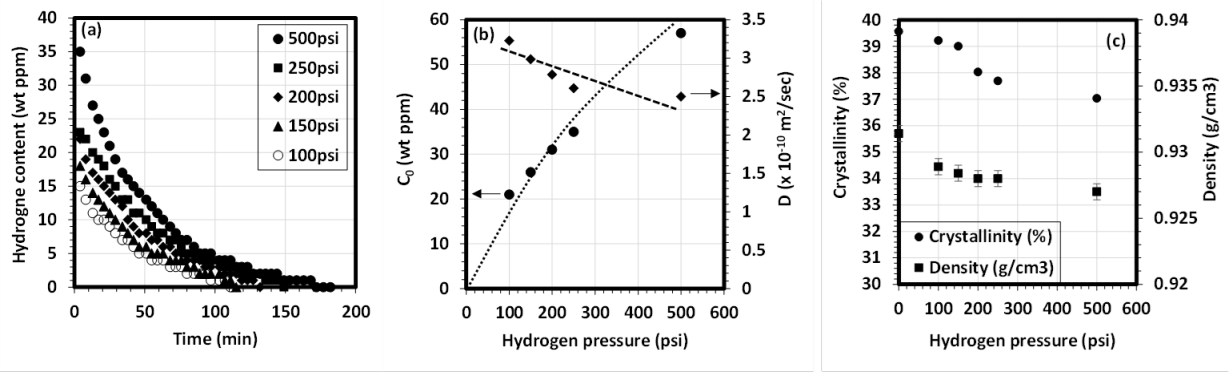


Figure 33. MDPE thermal desorption data.[41] (a) Desorption data, (b) pressure dependence of equilibrium hydrogen concentration and diffusion coefficient, and (c) crystallinity and density change post-decompression.

Temperature

The temperature dependence of the transport properties of polymers obeys classical Arrhenius's laws in a narrow temperature range[119], i.e.

$$A = A_0 exp\left(\frac{-E_a}{RT}\right) \quad (18)$$

where $A_0$ and $E_a$ are material-dependent constants and $A$ represents the transport property $P$, $D$, or $S$. This temperature dependence is followed for polymer materials at low pressures as long as the material's microstructure is not changing.[120] Figure 34 specifically shows the temperature-dependent permeability data from following this relationship well. It also shows that $E_a$ is roughly constant for this broad set of materials and that among all materials tested, polyamides (PA) and HDPE showed the lowest permeability and hence the best gas barrier properties.

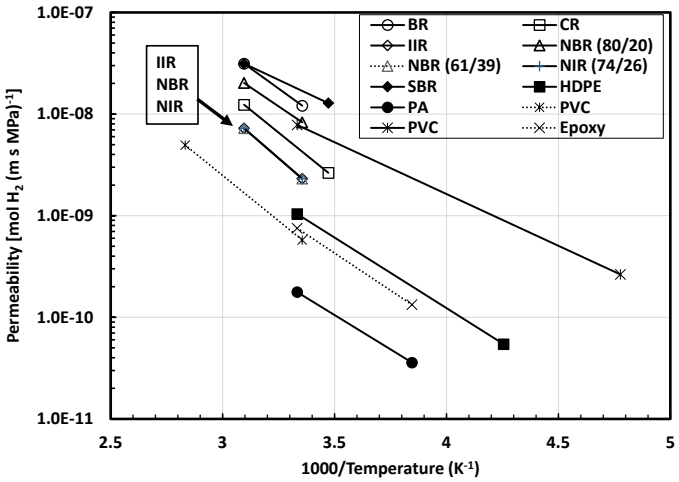


Figure 34. Temperature dependence of hydrogen permeability of polymer materials, modified with permission from ref. [120]

Crystallinity

Kane et al. demonstrated the influence of micro-crystallinity in PE on hydrogen permeability and showed that the higher the crystallinity, the stronger the barrier to hydrogen gas permeation.[82] Fujiwara et al.[41] investigated five different types of polyethylene: low-density polyethylene (LDPE), linear low-density polyethylene (LLDPE), medium-density polyethylene (MDPE), high-density polyethylene used in tank liners (HDPE), high-density polyethylene (PE 100), and ultra-high molecular weight polyethylene (UHMWPE). Each of these PEs was tested in the range of 5 to 90MPa hydrogen pressure under non-equilibrium conditions using TDA and under equilibrium conditions using the high-pressure hydrogen gas permeation test (HPHP) to elucidate the effect of physical properties on hydrogen permeability. The experimental results show that hydrogen gas penetrates into the amorphous region of polymers under high-pressure conditions. PE polymers with higher crystallinity show increased barrier properties to hydrogen gas, as illustrated in Figure 35.

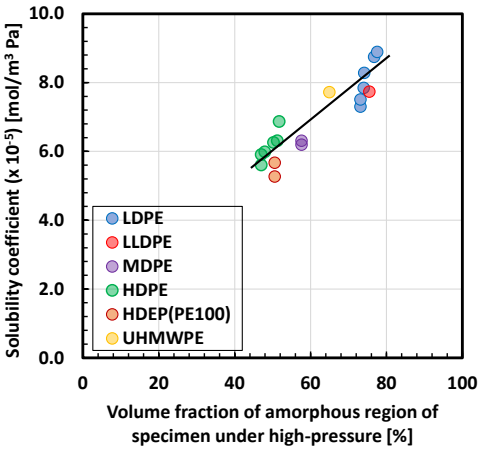


Figure 35. Effect of crystallinity in different PE polymers on hydrogen solubility in a high-pressure gas environment, reproduced with permission from ref.[41]

#### 3.3.1.5 Additives

Additives such as crosslinking agents, plasticizers, processing aids, and fillers are often added to polymer materials to attain properties that are needed in the polymer manufacturing process or to meet the target properties of the material. These additives can affect the gas barrier properties of the PE polymers. The addition of crosslinking agents will change the degree of cross-linking between molecular chains, affect the gaps between molecular chains, and thereby affect the penetration of gas molecules. The higher the degree of crosslinking, the more difficult it is for molecular chains to move and for penetrants with a diameter larger than the cross-linking gap to diffuse. Plasticizers slightly modify the hydrogen permeability in PE polymers because they weaken the interaction between polymer molecular chains and give molecular chains more freedom to move. While plasticizers are not a typical additive in PE pipe materials, some substances, such as hydrocarbon gases, may have a plasticizing effect on the PE material during service.

The effect of crosslinking agents and plasticizers on the hydrogen permeability of PE polymers is rarely reported. The addition of fillers to PE polymers as an additive has shown to improve its gas barrier properties. In one report, a 10% increase in clay loading in PE resulted in three times reduced helium gas permeability.[121] The barrier properties of HDPE nanocomposites are directly related to the clay dispersion state but also derive from the PE/clay interfacial interactions.[122] Oxidized wax was found to be a very promising interfacial agent, and the combination of PE and middle molar mass oxidized PE (mwOX16) performed better as a hydrogen barrier than neat HDPE due to its relatively hydrophilic characteristics (Figure 36).

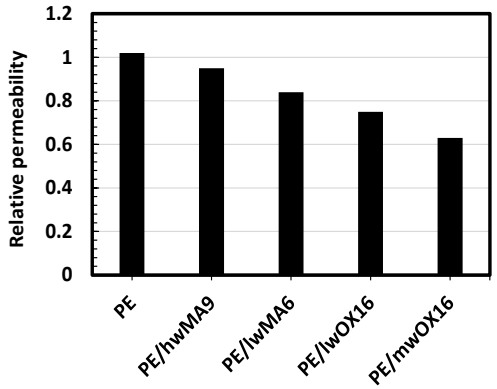


Figure 36. Relative hydrogen permeability values for PE-based nanocomposite films prepared with different fillers. Modified with permission from ref.[122]

In summary, this section has discussed the principles of permeability, diffusivity, and solubility of hydrogen gas in PEs and some specific factors in their variability, as evidenced in the technical literature. However, these studies do not yet provide comprehensive detail relative to polymer morphology and chemistry, crystallinity and homogeneity, degree of oxidation, and polymer chain orientation in PEs. Moreover, the literature is in a primitive state relative to gas mixtures of hydrogen with natural gas. Additional studies are needed that would help generalize our understanding of these materials and improve predictive models of hydrogen permeation phenomena for PE materials.

## 3.4 Analysis and Key Take-Aways on Chemical, Mechanical, Physical, and Transport Properties for Pipelines of Blended Hydrogen and Natural Gas

Having reviewed the existing data on mechanical, chemical, physical, and permeation properties of polyethylene pipeline materials exposed to hydrogen and hydrogen blends, several aspects have been identified that should be considered before introducing hydrogen blends into the natural gas distribution system.

Mechanical Properties:

While the global elastic modulus of PE measured from uniaxial tensile tests is less affected by hydrogen pressure up to about 5076 psi (35 MPa), the local elastic modulus, as well as hardness, can be affected up to 10-30% by hydrogen measured through nanoindentation. Nanoindentation data on PE materials exposed to hydrogen and hydrogen blends at the operating conditions of the pipeline should be collected. Also, understanding the relationship between this property change and the long-term performance of the material is needed

Both stress and strain at the first peak load of HDPE from uniaxial tensile tests decrease slightly (up to 15%) as the hydrogen pressure increases up to 5076 psi (35 MPa). Whether this phenomenon is due to hydrogen or to pressure alone remains unclear. Additional testing is needed to investigate pressure effects separate from hydrogen effects. Stresses at the first peak load of HDPE from ex-situ uniaxial tensile tests at different temperatures from 20 to 80°C are not significantly affected by hydrogen at a pressure of 3 MPa. This is positive but doesn't extend to the operating temperature minimum of -29°C, and it is only one data set. Data sets should be collected that include the minimum operating temperature and hydrogen blend gas. Additionally, hydrogen effects on the PE materials under multi-axial stress state needs more investigations in the future since the PE pipes are always under multi-axial stress states in service. This testing should be performed in situ.

By scaling up from coupon level testing to actual pipe specimens, hydrostatic burst pressure, maximum principal strain at the failure location, and fracture morphology are also not significantly affected by hydrogen exposure. However, these ex-situ measurements are time-dependent, and data taken long after exposure may recover and not be commensurate with actual operating conditions. Burst testing with hydrogen and hydrogen blend gas as the pressurizing gas should be completed.

In the case of HDPE in the presence of a pre-existing notch, the Mode I fracture energy and dissipation are not significantly affected by hydrogen (pressure = 435 psi (3 MPa)), but again this is only one data set. Data is needed on hydrogen effects on other modes of fracture because they involve different deformation processes that may be more sensitive to hydrogen. Additional data sets should be generated on hydrogen blend gas effects on the slow crack growth in PE materials in fatigue and creep conditions with a sharp notch since the local material degradation/change ahead of notch tip due to hydrogen potentially affects the foregoing long-term mechanical behavior. This testing should be performed in-situ.

In terms of long-term mechanical performance, hydrogen does not significantly affect fatigue tensile behavior by showing similar stress-life curves obtained from circumferential notched tensile specimens. This is also true for creep behavior of HDPE at low stress level (5 MPa) by showing similar strain evolutions under air and hydrogen (pressure = 435 psi (3 MPa)) conditions obtained by leveraging TTS method. However, it is difficult to draw a solid condition for negligible hydrogen effect on the long-term mechanical behavior mainly due to the following reasons: (1) the data reviewed in this study was not pure experimental results but reconstructed from accelerated experiments at higher temperatures; (2) hydrogen effect on the creep behavior of PE materials under various constant stress levels was not explored in the literature. There is a need for additional in-situ fatigue and creep testing in hydrogen blend gas at various stress levels.

Chemical Degradation:

There is very little data on material degradation induced by hydrogen on PE pipes. One dataset based on a study of PE pipes in Denmark showed no change in OIT after four years of exposure to hydrogen at 4 barg and 8°C. No other data has been reported under different environmental conditions, such as temperature, pressure, humidity, UV radiation, and concentration of contaminants in the gas. Data should be collected on hydrogen effects on the OIT of pipeline materials at the operating and environmental conditions experienced in service, with a priority on temperature and gas contaminants.

The heat fusion joining process requires high temperatures under which the antioxidants could be depleted. Depletion of antioxidants can cause changes to the fracture toughness and crack propagation over time. While this is an issue even for natural gas, hydrogen addition is not well understood on whether it could contribute to increased depletion rates. No OIT data was found on heat fusion joints, neither exposed or not exposed to hydrogen. The OIT profile of heat fusion joints needs to be established along the longitudinal direction of the pipe and through the wall thickness to determine the affected region. Pipes may be exposed to hydrogen prior to the joining operation, and it is not known if this exposure will cause voids or other unacceptable defects in the joint zone. The effects of hydrogen exposure on an already existing heat fusion joint is another area that requires investigation. As previously discussed, the joint zone may have depleted antioxidants and it may be more susceptible to hydrogen effects.

Physical Properties:

The magnitude of changes in physical properties of PE, including density and crystallinity as a function of exposed pressure, are initial material density-dependent and are reversible after decompression. Test data on physical changes in hydrogen blended gas was not found.

There is a need to utilize non-destructive imaging technologies, such as X-ray CT, to further understand hydrogen effects on internal wall damage and crack initiation geometries. Most studies on the effect of hydrogen on PE materials have been limited to a macroscopic understanding of crystallinity, density, and free volume. A molecular-level understanding of crystallite morphology will be beneficial in understanding the failure of pipe materials. In addition, studies correlating nondestructive techniques like light transmission and X-ray CT with macroscopic tensile, flexural, and fatigue testing are warranted.

Hydrogen Losses Through Pipeline Permeation:

Hydrogen permeation rates are important to the transition to a hydrogen economy from environmental and economic aspects. However, estimating hydrogen permeation rates and losses is very challenging due to lack of existing data and effective measuring techniques. Also, lack of understanding in the relationship between transport properties and leakage rate is a hurdle for accurately evaluating hydrogen loss at large scales and longer terms. In addition to permeation through pipeline walls and heat fusion joints, other factors to consider for hydrogen loss are mechanical joints and valves.

Even though various factors on the hydrogen permeation of PE materials have been investigated, there is still a lack of understanding of effects of crystallinity and its homogeneity, degree of oxidation, and macromolecular chain orientation on hydrogen permeation in the PE materials. There is also a lack of data on the permeation of hydrogen gas blended with natural gas. The amount of hydrogen that permeates (leaks) through the pipe could have safety, cost, and environmental consequences.

The evaluated hydrogen permeation data should be further analyzed, and a general prediction model should be implemented based on the hydrogen and hydrogen blend permeation phenomena of PE materials to correlate with physical and mechanical properties in a hydrogen environment.

# 4.0 Conclusions and Recommendations

In summary, we have reviewed the existing standards and data related to the effects of hydrogen and natural gas blends on polyethylene pipeline materials. This review identified the major gaps in data and what testing and development is still needed to determine the effects on pipeline lifetime when hydrogen is blended with natural gas.

- In all aspects investigated for this review, there was no data found on the effects of hydrogen gas blended with natural gas on plastic piping? The test data found during this review utilized pure hydrogen. The data reviewed using pure hydrogen was very limited, and the majority of it was short term type testing. Refer to section 3.0

- While the existing data suggests hydrogen effects are small, the correlation of these small changes to long term performance must be evaluated. Testing of hydrogen blend gas on the slow crack growth of pipeline materials under in-service conditions is needed. Refer to sections 2.3.2, 2.4, and 3.1

- It is also evident from the review that there is a future need to revise or create new codes and standards (including test methodologies) to address the requirements for blending hydrogen into the natural gas pipelines. Refer to section 2.2

- Investigation into the permeation of hydrogen gas blend through the polyethylene pipeline system to evaluate safety, cost, and environmental impacts of gas leakage rates is warranted. Refer to section 3.3

Based on this review, it is recommended that work continue in the effort to evaluate the effects of hydrogen blend gas on polyethylene pipeline materials in regards to both material degradation and gas permeation since these pipelines are such a critical part of the infrastructure. The specific recommendations for further investigation are detailed in Sections 2.5 and 3.4.

# 5.0 References


1. Celestine, A.-D. N.; Sulic, M.; Wieliczko, M.; Stetson, N. T., Hydrogen-Based Energy Storage Systems for Large-Scale Data Center Applications. *Sustainability* **2021,** *13* (22), 12654.
2. Moon, S.; Lee, Y.; Seo, D.; Lee, S.; Hong, S.; Ahn, Y.-H.; Park, Y., Critical hydrogen concentration of hydrogen-natural gas blends in clathrate hydrates for blue hydrogen storage. *Renewable and Sustainable Energy Reviews* **2021,** *141*, 110789.
3. Gondal, I. A., Hydrogen integration in power-to-gas networks. *International journal of hydrogen energy* **2019,** *44* (3), 1803-1815.
4. Gondal, I., Hydrogen transportation by pipelines. In *Compendium of Hydrogen Energy*, Elsevier: 2016; pp 301-322.
5. BLANTON, E. M.; LOTT, D. M. C.; Smith, K. N., Investing in the US Natural Gas Pipeline System to Support Net-Zero Targets. *Center on Global Energy Policy, Columbia University, April* **2021**.
6. Ahn, D.; Sofronis, P.; Dodds, R., Modeling of hydrogen-assisted ductile crack propagation in metals and alloys. *International Journal of Fracture* **2007,** *145* (2), 135-157.
7. Hirth, J. P., Effects of hydrogen on the properties of iron and steel. *Metallurgical Transactions A* **1980,** *11* (6), 861-890.
8. Michler, T.; Elsässer, C.; Wackermann, K.; Schweizer, F., Effect of Hydrogen in Mixed Gases on the Mechanical Properties of Steels—Theoretical Background and Review of Test Results. *Metals* **2021,** *11* (11), 1847.
9. Wu, X.; Zhang, H.; Yang, M.; Jia, W.; Qiu, Y.; Lan, L., From the perspective of new technology of blending hydrogen into natural gas pipelines transmission: Mechanism, experimental study, and suggestions for further work of hydrogen embrittlement in high-strength pipeline steels. *International Journal of Hydrogen Energy* **2022**.
10. Castagnet, S.; Grandidier, J.-C.; Comyn, M.; Benoît, G., Effect of long-term hydrogen exposure on the mechanical properties of polymers used for pipes and tested in pressurized hydrogen. *International Journal of Pressure Vessels and Piping* **2012,** *89*, 203-209.
11. Castagnet, S.; Grandidier, J.-C.; Comyn, M.; Benoît, G., Hydrogen influence on the tensile properties of mono and multi-layer polymers for gas distribution. *International Journal of Hydrogen Energy* **2010,** *35* (14), 7633-7640.
12. Iskov, H., Field test of hydrogen in the natural gas grid. **2010**.
13. Radoszewski, T., Plastic Pipe Where Past is Prelude. *Pipeline and Gas Journal* **2014,** *241* (12).
14. DesLauriers, P. J.; McDaniel, M. P.; Rohlfing, D. C.; Krishnaswamy, R. K.; Secora, S. J.; Benham, E. A.; Maeger, P. L.; Wolfe, A.; Sukhadia, A. M.; Beaulieu, B. B., A comparative study of multimodal vs. bimodal polyethylene pipe resins for PE-100 applications. *Polymer Engineering & Science* **2005,** *45* (9), 1203-1213.
15. DOW CONTINUUM DGDA-2420 Bimodal MDPE Resin Technical Datasheet. Plastics, D., Ed. 2016.
16. Moidel, B. *PE 2708 Medium Density Bi-Modal PE Materials*; Dominion East Ohio Gas: 2011.
17. Handbook of Polyethylene Pipe. Plastic Pipe Institute: 2008.
18. Barber, P.; Atkinson, J., Some microstructural features of the welds in butt-welded polyethylene and polybutene-1 pipes. *Journal of Materials Science* **1972,** *7* (10), 1131-1136.
19. Gunther, K., Fusion, mechanical joining methods pros, cons--Part 2.[Natural gas pipelines use of mechanical and fusion joints]. *Pipe Line Industry;(United States)* **1993,** *76* (10).
20. 2020 Annual Report Data from Gas Distribution, Gas Gathering, Gas Transmission, Hazardous Liquids, Liquefied Natural Gas (LNG), and Underground Natural Gas Storage (UNGS) Facility Operators. USDOT, P., Ed. 2020; Vol. 2022.

21. Distribution, Transmission & Gathering, LNG, and Liquid Accident and Incident Data. USDOT, P., Ed. 2020.
22. Steven Haine, P. E. *Hazard Analysis & Mitigation Report On Aldyl A Polyethylene Gas Pipelines in California*; California Public Utilities Commisssion: June 11, 2014, 2014.
23. Plastic Pipe Database Collection Initiative. https://www.aga.org/safety/promoting-safety/plastic-pipe-database-collection-initiative/.
24. Mamoun, M. M.; Maupin, J. K.; Miller, M. J. *Plastic Pipe Failure, Risk, and Threat Analysis*; 2009.
25. Krishnaswamy, R. K., Analysis of ductile and brittle failures from creep rupture testing of high-density polyethylene (HDPE) pipes. *Polymer* **2005,** *46* (25), 11664-11672.
26. Chaoui, K.; Khelif, R.; Zeghib, N.; Chateauneuf, A. In *Failure Analysis of Polyethylene Gas Pipes*, Safety, Reliability and Risks Associated with Water, Oil and Gas Pipelines, Dordrecht, 2008//; Pluvinage, G.; Elwany, M. H., Eds. Springer Netherlands: Dordrecht, 2008; pp 131-163.
27. O'Connor, C.; Denton, G. N. In *Polyethylene pipeline systems: Avoiding the pitfalls of fusion welding*, Proceedings of the 7th Pipeline Technology Conference, Hannover, Germany, 2012; pp 28-30.
28. Parsons, M.; Stepanov, E.; Hiltner, A.; Baer, E., Correlation of fatigue and creep slow crack growth in a medium density polyethylene pipe material. *Journal of materials science* **2000,** *35* (11), 2659-2674.
29. Huang, Y. L.; Brown, N., The effect of molecular weight on slow crack growth in linear polyethylene homopolymers. *Journal of Materials Science* **1988,** *23* (10), 3648-3655.
30. Adib, A.; Domínguez, C.; Rodríguez, J.; Martín, C.; García, R. A., The effect of microstructure on the slow crack growth resistance in polyethylene resins. *Polymer Engineering & Science* **2015,** *55* (5), 1018-1023.
31. Huang, Y. L.; Brown, N., Dependence of slow crack growth in polyethylene on butyl branch density: morphology and theory. *Journal of Polymer Science Part B: Polymer Physics* **1991,** *29* (1), 129-137.
32. Lu, X.; Brown, N., A test for slow crack growth failure in polyethylene under a constant load. *Polymer Testing* **1992,** *11* (4), 309-319.
33. Brown, H., A molecular interpretation of the toughness of glassy polymers. *Macromolecules* **1991,** *24* (10), 2752-2756.
34. Hui, C.; Ruina, A.; Creton, C.; Kramer, E., Micromechanics of crack growth into a craze in a polymer glass. *Macromolecules* **1992,** *25* (15), 3948-3955.
35. Domínguez, C.; Robledo, N.; Paredes, B.; García-Muñoz, R. A., Strain hardening test on the limits of Slow Crack Growth evaluation in high resistance polyethylene resins: Effect of comonomer type. *Polymer Testing* **2020,** *81*, 106155.
36. Melaina, M. W.; Antonia, O.; Penev, M., Blending hydrogen into natural gas pipeline networks: a review of key issues. **2013**.
37. Alvine, K. J.; Kafentzis, T. A.; Pitman, S. G.; Johnson, K. I.; Skorski, D.; Tucker, J. C.; Roosendaal, T. J.; Dahl, M. E., An in situ tensile test apparatus for polymers in high pressure hydrogen. *Review of Scientific Instruments* **2014,** *85* (10), 105110.
38. Klopffer, M.-H.; Berne, P.; Castagnet, S.; Weber, M.; Hochstetter, G.; Espuche, E. In *Polymer pipes for distributing mixtures of hydrogen and natural gas. Evolution of their transport and mechanical properties after an ageing under an hydrogen environment*, Germany, 2010-07-01; Germany, 2010.
39. Kevin L Simmons, L. F., Wenbin Kuang, Yongsoon Shin, Rakish Shrestha, Chris San Marchi In *Morphological Changes and Their Effects on Material Properties in Natural Gas Medium Density Polyethylene Pipe in Low Pressure Hydrogen* Materials Research Society (MRS 2021), Virtual, MRS 2021: Virtual, 2021.

40. Menon, N. C.; Kruizenga, A. M.; Alvine, K. J.; San Marchi, C.; Nissen, A.; Brooks, K. In *Behaviour of polymers in high pressure environments as applicable to the hydrogen infrastructure*, Pressure Vessels and Piping Conference, American Society of Mechanical Engineers: 2016; p V06BT06A037.
41. Fujiwara, H.; Ono, H.; Ohyama, K.; Kasai, M.; Kaneko, F.; Nishimura, S., Hydrogen permeation under high pressure conditions and the destruction of exposed polyethylene-property of polymeric materials for high-pressure hydrogen devices (2). *International Journal of Hydrogen Energy* **2021,** *46* (21), 11832-11848.
42. Castagnet, S.; Grandidier, J.-C.; Comyn, M.; Benoît, G., Mechanical testing of polymers in pressurized hydrogen: tension, creep and ductile fracture. *Experimental mechanics* **2012,** *52* (3), 229-239.
43. Simmons K.L., C. W. S. M., L.D. Fring, Y. Shin, Y. Qiao, R. Shrestha, and W. Kuang, et al., Hydrogen Infrastructure Assessment for Injection of Gaseous Hydrogen in Atlanta Gas Light Company (AGLC) Natural Gas Distribution Lines. Pacific Northwest National Laboratory: 2022.
44. Shaheer, M.; Troughton, M.; Khamsehnezhad, A.; Song, J., A study of the micro-mechanical properties of butt fusion-welded joints in HDPE pipes using the nanoindentation technique. *Welding in the World* **2017,** *61* (4), 819-831.
45. Chen, S.; Lai, H. S.; Lin, R.; Duan, X. H., Study on the creep properties of butt fusion–welded joints of HDPE pipes using the nanoindentation test. *Welding in the World* **2022,** *66* (1), 135-144.
46. Abdelkader, D.; Mostefa, B.; Abdelkrim, A.; Abderrahim, T.; Noureddine, B.; Mohamed, B., Fatigue life prediction and damage modelling of high-density polyethylene under constant and two-block loading. *Procedia Engineering* **2015,** *101*, 2-9.
47. Van Gurp, M.; Palmen, J., Time-temperature superposition for polymeric blends. *Rheol. Bull* **1998,** *67* (1), 5-8.
48. Zornberg, J. G.; Byler, B. R.; Knudsen, J. W., Creep of geotextiles using time–temperature superposition methods. *Journal of geotechnical and geoenvironmental engineering* **2004,** *130* (11), 1158-1168.
49. Dear, J. P.; Mason, N. S., The Effects of Chlorine Depletion of Antioxidants in Polyethylene. *Polymers and Polymer Composites* **2001,** *9* (1), 1-13.
50. Castagnetti, D.; Mammano, G. S.; Dragoni, E., Effect of chlorinated water on the oxidative resistance and the mechanical strength of polyethylene pipes. *Polymer testing* **2011,** *30* (3), 277-285.
51. Hassinen, J.; Lundbäck, M.; Ifwarson, M.; Gedde, U., Deterioration of polyethylene pipes exposed to chlorinated water. *Polymer degradation and stability* **2004,** *84* (2), 261-267.
52. Choi, B.-H.; Chudnovsky, A.; Sehanobish, K., Stress corrosion cracking in plastic pipes: observation and modeling. *International Journal of Fracture* **2007,** *145* (1), 81-88.
53. Pinter, G.; Lang, R., Effect of stabilization on creep crack growth in high-density polyethylene. *Journal of applied polymer science* **2003,** *90* (12), 3191-3207.
54. Segrestin, P.; Jailloux, J., Temperature in soils and its effect on the ageing of synthetic materials. *Geotextiles and Geomembranes* **1988,** *7* (1/2).
55. Khajehpour, M.; Wong, F.; Huizing, R.; Bahrami, M., Longevity of Membrane for Energy Recovery Ventilation: Thermal, Humidity, and Oxygen Stability.
56. Krushelnitzky, R.; Brachman, R., Antioxidant depletion in high-density polyethylene pipes exposed to synthetic leachate and air. *Geosynthetics International* **2011,** *18* (2), 63-73.
57. Jeon, H.-Y.; Bouazza, A.; Lee, K.-Y., Depletion of antioxidants from an HDPE geomembrane upon exposure to acidic and alkaline solutions. *Polymer Testing* **2008,** *27* (4), 434-440.
58. Erdmann, M.; Niebergall, U.; Wachtendorf, V.; Böhning, M., Evaluation of UV-induced embrittlement of PE-HD by Charpy impact test. *Journal of Applied Polymer Science* **2020,** *137* (36), 49069.

59. Sen, M.; Basfar, A., The effect of UV light on the thermooxidative stability of linear low density polyethylene films crosslinked by ionizing radiation. *Radiation Physics and Chemistry* **1998,** *52* (1-6), 247-250.
60. Viebke, J.; Gedde, U., Antioxidant diffusion in polyethylene hot-water pipes. *Polymer Engineering & Science* **1997,** *37* (5), 896-911.
61. Bachir-Bey, T.; Belhaneche-Bensemra, N., Investigation of Polyethylene Pipeline Behavior after 30 Years of Use in Gas Distribution Network. *Journal of Materials Engineering and Performance* **2020,** *29* (10), 6652-6660.
62. https://www.climatestotravel.com/climate/algeria.
63. De Silva, R.; Hilditch, T.; Byrne, N., Assessing the integrity of in service polyethylene pipes. *Polymer Testing* **2018,** *67*, 228-233.
64. Byrne, N.; De Silva, R.; Hilditch, T., Linking Antioxidant Depletion with Material Properties for Polyethylene Pipes Resins. *Polymer Engineering & Science* **2020,** *60* (2), 323-329.
65. Celina, M.; Elliott, J. S.; Winters, S.; Assink, R.; Minier, L., Correlation of antioxidant depletion and mechanical performance during thermal degradation of an HTPB elastomer. *Polymer degradation and stability* **2006,** *91* (8), 1870-1879.
66. Pospíšil, J., Chemical and photochemical behaviour of phenolic antioxidants in polymer stabilization—a state of the art report, Part I. *Polymer Degradation and stability* **1993,** *40* (2), 217-232.
67. Nolene Byrne, R. D. S., Keith Lenghaus, Tim Hilditch In *Assessing the remaining service lifetime of PE pipes: an australian case study*, Plastic Pipes Conference Association, Las Vegas, Plastic Pipes Conference Association: Las Vegas, 2018.
68. Latocha, C.; Uhniat, M., The kinetics of oxidative induction of LDPE stabilized with commercial antioxidants. *Polymer degradation and stability* **1992,** *35* (1), 17-22.
69. Földes, E., Transport of small molecules in polyolefins. II. Diffusion and solubility of irganox 1076 in ethylene polymers. *Journal of applied polymer science* **1993,** *48* (11), 1905-1913.
70. Wang, Y.; Lan, H.-q.; Meng, T.; Wang, B.; Guo, D.-d.; Zhuang, L.-j., Pressure Effects on the Lifetime of Gas High Density Polyethylene Pipes. *Journal of Pressure Vessel Technology* **2022,** *144* (2).
71. Bondet, V.; Brand-Williams, W.; Berset, C., Kinetics and mechanisms of antioxidant activity using the DPPH. free radical method. *LWT-Food Science and Technology* **1997,** *30* (6), 609-615.
72. Calvert, P.; Billingham, N., Loss of additives from polymers: a theoretical model. *Journal of Applied Polymer Science* **1979,** *24* (2), 357-370.
73. Verdu, J., *Oxydative ageing of polymers*. John Wiley & Sons: 2012.
74. Djouani, F.; Patel, B.; Richaud, E.; Fayolle, B.; Verdu, J., Antioxidants loss kinetics in polyethylene exposed to model ethanol based biofuels. *Fuel* **2012,** *93*, 502-509.
75. Haider, N.; Karlsson, S., Kinetics of migration of antioxidants from polyolefins in natural environments as a basis for bioconversion studies. *Biomacromolecules* **2000,** *1* (3), 481-487.
76. Rashid, H. Butt fusion welding of polyethylene pipes. Brunel University, Uxbridge, 1997.
77. Šimon, P.; Hynek, D.; Malíková, M.; Cibulková, Z., Extrapolation of accelerated thermooxidative tests to lower temperatures applying non-Arrhenius temperature functions. *Journal of thermal analysis and calorimetry* **2008,** *93* (3), 817-821.
78. Celina, M.; Gillen, K. T.; Assink, R., Accelerated aging and lifetime prediction: Review of non-Arrhenius behaviour due to two competing processes. *Polymer Degradation and stability* **2005,** *90* (3), 395-404.
79. Shlyapnikov, Y. A., Physical chemistry of topological disorder in polymers. Some comments on reactions kinetics of low-molecular antioxidants. *European polymer journal* **1998,** *34* (8), 1177-1184.
80. Gugumus, F., Critical antioxidant concentrations in polymer oxidation—III. Application to lifetime prediction∗. *Polymer degradation and stability* **1998,** *60* (1), 119-135.

81. Craig, B., Hydrogen damage. **2003**.
82. Kane, M. *Permeability, solubility, and interaction of hydrogen in polymers-An assessment of materials for hydrogen transport*; Savannah River Site (SRS), Aiken, SC (United States): 2008.
83. Mokhatab, S.; Poe, W. A.; Mak, J. Y., Chapter 3-Basic Concepts of Natural Gas Processing. Handbook of Natural Gas Transmission and Processing. Boston: Gulf Professional Publishing: 2015.
84. Dörner, G.; Lang, R., Influence of various stabilizer systems on the ageing behavior of PE–MD—II. Ageing of pipe specimens in air and water at elevated temperatures. *Polymer Degradation and Stability* **1998,** *62* (3), 431-440.
85. Leskovics, K.; Kollár, M.; Bárczy, P., A study of structure and mechanical properties of welded joints in polyethylene pipes. *Materials Science and Engineering: A* **2006,** *419* (1-2), 138-143.
86. Nishimura, H.; Narisawa, I., Evaluation of impact properties of butt-fusion-jointed medium-density polyethylene pipes for gas distribution. *Polymer* **1991,** *32* (12), 2199-2204.
87. Tariq, F.; Naz, N.; Khan, M. A.; Baloch, R. A., Failure analysis of high density polyethylene butt weld joint. *Journal of failure analysis and prevention* **2012,** *12* (2), 168-180.
88. Kong, Y.; Hay, J., The enthalpy of fusion and degree of crystallinity of polymers as measured by DSC. *European Polymer Journal* **2003,** *39* (8), 1721-1727.
89. Segal, L.; Creely, J. J.; Martin Jr, A.; Conrad, C., An empirical method for estimating the degree of crystallinity of native cellulose using the X-ray diffractometer. *Textile research journal* **1959,** *29* (10), 786-794.
90. Nielsen, L. E., Effect of crystallinity on the dynamic mechanical properties of polyethylenes. *Journal of Applied Physics* **1954,** *25* (10), 1209-1212.
91. Frank, A.; Pinter, G.; Lang, R., Prediction of the remaining lifetime of polyethylene pipes after up to 30 years in use. *Polymer Testing* **2009,** *28* (7), 737-745.
92. Fujiwara, H.; Ono, H.; Onoue, K.; Nishimura, S., High-pressure gaseous hydrogen permeation test method-property of polymeric materials for high-pressure hydrogen devices (1). *International Journal of Hydrogen Energy* **2020,** *45* (53), 29082-29094.
93. Fujiwara, H.; Ono, H.; Onoue, K.; Nishimura, S., High-pressure gaseous hydrogen permeation test method -property of polymeric materials for high-pressure hydrogen devices (1). *International Journal of Hydrogen Energy* **2020,** *45* (53), 29082-29094.
94. Ono, H.; Fujiwara, H.; Onoue, K.; Nishimura, S., Influence of repetitions of the high-pressure hydrogen gas exposure on the internal damage quantity of high-density polyethylene evaluated by transmitted light digital image. *International Journal of Hydrogen Energy* **2019,** *44* (41), 23303-23319.
95. Yampolskii, Y. P., Methods for investigation of the free volume in polymers. *Russian chemical reviews* **2007,** *76* (1), 59.
96. Park, J.; Paul, D., Correlation and prediction of gas permeability in glassy polymer membrane materials via a modified free volume based group contribution method. *Journal of Membrane Science* **1997,** *125* (1), 23-39.
97. Gupta, S., *Practical density measurement and hydrometry*. CRC Press: 2002.
98. **!!! INVALID CITATION !!! 115**.
99. Ocko, I. B.; Hamburg, S. P., Climate consequences of hydrogen leakage. *Atmospheric Chemistry and Physics Discussions* **2022**, 1-25.
100. Kammen, D. M.; Lipman, T. E.; Lovins, A. B.; Lehman, P. A.; Eiler, J. M.; Tromp, T. K.; Shia, R.-L.; Allen, M.; Yung, Y., Assessing the future hydrogen economy. *Science* **2003,** *302* (5643), 226-229.
101. Darcy, H., *Les fontaines publiques de la ville de Dijon: Exposition et application des principes à suivre et des formules à employer dans les questions de distribution d'eau: Ouvrage terminé par un appendice relatif aux fournitures d'eau de plusieurs villes, au filtrage des eaux et à la fabrication des tuyaux de fonte, de plomb, de tôle et de bitume*. V. Dalmont: 1856; Vol. 2.

102. Klopffer, M.-H.; Berne, P.; Espuche, É., Development of innovating materials for distributing mixtures of hydrogen and natural gas. Study of the barrier properties and durability of polymer pipes. *Oil & Gas Science and Technology–Revue d'IFP Energies nouvelles* **2015,** *70* (2), 305-315.
103. Miyake, H.; Matsuyama, M.; Ashida, K.; Watanabe, K., Permeation, diffusion, and solution of hydrogen isotopes, methane, and inert gases in/through tetrafluoroethylene and polyethylene. *Journal of Vacuum Science & Technology A: Vacuum, Surfaces, and Films* **1983,** *1* (3), 1447-1451.
104. Administration, U. E. I., Government Printing Office: 2021.
105. Quality, N. D. o. E. *Nebraska's Keystone XL Pipeline Evaluation*; 2012.
106. Miyake, A.; Friedman, N. P., Individual differences in second language proficiency: Working memory as language aptitude. *Foreign language learning: Psycholinguistic studies on training and retention* **1998**, 339-364.
107. Klopffer, M.; Flaconneche, B., Transport properties of gases in polymers: bibliographic review. *Oil & Gas Science and Technology* **2001,** *56* (3), 223-244.
108. **!!! INVALID CITATION !!! 92-94**.
109. Jung, J. K.; Kim, I. G.; Kim, K., Evaluation of hydrogen permeation characteristics in rubbery polymers. *Current Applied Physics* **2021,** *21*, 43-49.
110. Jung, J. K.; Kim, I. G.; Chung, K. S.; Kim, Y.-I.; Kim, D. H., Determination of permeation properties of hydrogen gas in sealing rubbers using thermal desorption analysis gas chromatography. *Scientific Reports* **2021,** *11* (1), 1-14.
111. Su, Y.; Lv, H.; Zhou, W.; Zhang, C., Review of the Hydrogen Permeability of the Liner Material of Type IV On-Board Hydrogen Storage Tank. *World Electric Vehicle Journal* **2021,** *12* (3), 130.
112. Rudawska, A., *Surface Treatment in Bonding Technology*. Academic Press: 2019.
113. Yamabe, J.; Nishimura, S., Influence of fillers on hydrogen penetration properties and blister fracture of rubber composites for O-ring exposed to high-pressure hydrogen gas. *International Journal of Hydrogen Energy* **2009,** *34* (4), 1977-1989.
114. Naito, Y.; Mizoguchi, K.; Terada, K.; Kamiya, Y., The effect of pressure on gas permeation through semicrystalline polymers above the glass transition temperature. *Journal of Polymer Science Part B: Polymer Physics* **1991,** *29* (4), 457-462.
115. Sakamoto, J.; Sato, R.; Nakayama, J.; Kasai, N.; Shibutani, T.; Miyake, A., Leakage-type-based analysis of accidents involving hydrogen fueling stations in Japan and USA. *International journal of hydrogen energy* **2016,** *41* (46), 21564-21570.
116. Honselaar, M.; Pasaoglu, G.; Martens, A., Hydrogen refuelling stations in the Netherlands: An intercomparison of quantitative risk assessments used for permitting. *international journal of hydrogen energy* **2018,** *43* (27), 12278-12294.
117. Li, N.; Long, R., Permeation through plastic films. *AIChE Journal* **1969,** *15* (1), 73-80.
118. Fumitoshi, K.; Hirotada, F.; Shin, N., Influence of high-pressure hydrogen gas on crystalline polymers. *Proceedings of the 33rd Polymer Degradation Discussion Group, St Julians, Malta* **2019**, 1-5.
119. George, S. C.; Thomas, S., Transport phenomena through polymeric systems. *Progress in Polymer science* **2001,** *26* (6), 985-1017.
120. Barth, R. R.; Simmons, K. L.; San Marchi, C. W. *Polymers for hydrogen infrastructure and vehicle fuel systems*; Sandia National Lab.(SNL-CA), Livermore, CA (United States); Pacific …: 2013.
121. Ebina, T.; Ishii, R.; Aizawa, T.; Yoshida, H., Development of clay-based film and its application to gas barrier layers of composite tanks. *Journal of the Japan Petroleum Institute* **2017,** *60* (3), 121-126.

122. Picard, E.; Gérard, J.-F.; Espuche, E., Reinforcement of the gas barrier properties of polyethylene and polyamide through the nanocomposite approach: key factors and limitations. *Oil & Gas Science and Technology–Revue d'IFP Energies nouvelles* **2015,** *70* (2), 237-249.

# 6.0 Acknowledgements

We would like to thank Jose Ramos for providing the pipe and joint images.

# Pacific Northwest National Laboratory

902 Battelle Boulevard
P.O. Box 999
Richland, WA 99354
1-888-375-PNNL (7665)

***www.pnnl.gov***